

# Effective Theory of ${}^3\text{H}$ and ${}^3\text{He}$

Sebastian König,<sup>1,\*</sup> Harald W. Griedhammer,<sup>2,†</sup> H.-W. Hammer,<sup>3,4,‡</sup> and U. van Kolck<sup>5,6,§</sup>

<sup>1</sup>*Department of Physics, The Ohio State University, Columbus, Ohio 43210, USA*

<sup>2</sup>*Institute for Nuclear Studies, Department of Physics,*

*George Washington University, Washington DC 20052, USA*

<sup>3</sup>*Institut für Kernphysik, Technische Universität Darmstadt, 64289 Darmstadt, Germany*

<sup>4</sup>*ExtreMe Matter Institute EMMI, GSI Helmholtzzentrum für  
Schwerionenforschung GmbH, 64291 Darmstadt, Germany*

<sup>5</sup>*Institut de Physique Nucléaire, CNRS/IN2P3,*

*Université Paris-Sud, 91406 Orsay, France*

<sup>6</sup>*Department of Physics, University of Arizona, Tucson, AZ 85721, USA*

(Dated: April 28, 2016)

## Abstract

We present a new perturbative expansion for pionless effective field theory with Coulomb interactions in which at leading order the spin-singlet nucleon–nucleon channels are taken in the unitarity limit. Presenting results up to next-to-leading order for the Phillips line and the neutron–deuteron doublet-channel phase shift, we find that a perturbative expansion in the inverse  ${}^1S_0$  scattering lengths converges rapidly. Using a new systematic treatment of the proton–proton sector that isolates the divergence due to one-photon exchange, we renormalize the corresponding contribution to the  ${}^3\text{H}$ – ${}^3\text{He}$  binding energy splitting and demonstrate that the Coulomb force in pionless EFT is a completely perturbative effect in the trinucleon bound-state regime. In our new expansion, the leading order is exactly isospin-symmetric. At next-to-leading order, we include isospin breaking via the Coulomb force and two-body scattering lengths, and find for the energy splitting  $(E_B({}^3\text{He}) - E_B({}^3\text{H}))^{\text{NLO}} = (-0.86 \pm 0.17) \text{ MeV}$ .

---

\*Electronic address: [koenig.389@osu.edu](mailto:koenig.389@osu.edu)

†Electronic address: [hgrie@gwu.edu](mailto:hgrie@gwu.edu)

‡Electronic address: [Hans-Werner.Hammer@physik.tu-darmstadt.de](mailto:Hans-Werner.Hammer@physik.tu-darmstadt.de)

§Electronic address: [vankolck@ipno.in2p3.fr](mailto:vankolck@ipno.in2p3.fr)

## I. INTRODUCTION

It has been known for a long time that two-nucleon ( $NN$ ) scattering at very low energies can be described by the effective range expansion [1], from which deuteron and  $^1S_0$  virtual state properties emerge without information about details of the strong interaction [2]. At these energies effects from pion-exchange physics cannot be resolved. It is therefore possible to describe such a system using only nonrelativistic nucleons as degrees of freedom that interact via short-range (contact) forces [3–12]. The systematic approach to implement this procedure, known as *pionless effective field theory* (pionless EFT), is based on the experimental fact that the  $NN$   $S$ -wave scattering lengths are much larger than the corresponding effective ranges, so that a nonperturbative resummation of non-derivative two-body contact interactions is required at leading order (LO) to reproduce the shallow  $NN$  bound and virtual states.

The extension of these ideas to the triton ( $^3\text{H}$ ) and helion ( $^3\text{He}$ ) was not immediate because a system of three nucleons collapses under the sole effect of attractive, non-derivative contact forces [13]. The solution within pionless EFT is the existence of a non-derivative three-body interaction [14–19] at LO. This force provides not only saturation, but also a three-body parameter which correlates certain observables such as the triton binding energy and the doublet neutron-deuteron ( $nd$ ) scattering length (“Phillips line” [20]). This framework recovers Efimov’s universal approach to the three-nucleon problem [21–23]. With recent progress, pionless EFT also allows for an elegant and efficient fully perturbative treatment of contributions beyond LO [16, 24–26].

An important question is how far up the nuclear chart this EFT applies. Nuclear density tends to increase with nucleon number  $A$ , implying larger typical nucleon momenta within the nucleus. Calculations suggest that pionless EFT holds for  $A = 4$  [27–30] and perhaps up to  $A = 6$  systems [30, 31] without a four-body force at LO. As the pion mass increases, its range of applicability increases, and this framework has been established as a powerful tool that can be used to analyze and supplement calculations of light nuclei directly from lattice QCD [32–34]. (See Refs. [35–37] for earlier work on pionless EFT for unphysical quark masses using input from chiral potentials.)

The application of EFT to nuclei requires an understanding of the importance of Coulomb and other electromagnetic effects. The long-range nature of the Coulomb force implies that it becomes dominant at very low energies, *i.e.*, precisely where the EFT is supposed to work best. To describe scattering in this regime, one thus has to resum Coulomb effects to all orders to recover the Coulomb-modified effective-range expansion. In the proton-proton ( $pp$ ) sector of the pionless theory this was first carried out by Kong and Ravnadal [38, 39], with subsequent discussions of the charged two-body sector given in Refs. [40–45]. An early attempt at  $pd$  scattering was made in Ref. [46], and extended to lower center-of-mass energies in Ref. [47]. A calculation of the Coulomb-modified  $pd$  scattering length, with the consistent use of a Yukawa-screened Coulomb potential in momentum space, has been presented in Ref. [25].

The  $^3\text{H}$ – $^3\text{He}$  binding energy difference has been studied using pionless EFT in a number of papers. Systems of three and four nucleons including the Coulomb interaction as part of an effective potential were first analyzed by Kirscher *et al.* using the resonating group method [28–30, 48]. Ando and Birse [49] carried out a momentum-space LO calculation which was nonperturbative both in the sense that it looked for the bound state as a pole in the  $pd$  doublet-channel amplitude, as well as in the electromagnetic sector, where Coulomb

effects were included through a fully off-shell Coulomb T-matrix, using methods developed by Kok *et al.* in Refs. [50, 51]. A subset of the present authors presented a calculation of  $pd$  scattering and the bound-state regime in Refs. [47, 52, 53]. Of these, Refs. [47, 52] included a perturbative framework using trinucleon wave functions. An updated version of this calculation that corrects some issues of the previous approach has recently been given in Ref. [54]. That work also includes a nonperturbative treatment, in which all  $\mathcal{O}(\alpha)$  Coulomb diagrams are resummed to all orders. This calculation was similar to that of Ref. [49] but found that the full Coulomb T-matrix is not necessary for an accurate description of the  ${}^3\text{He}$  bound state.

At LO in the strong interactions, the perturbative and nonperturbative results of Ref. [54] were found to agree with each other (as well as with the experimental value for the  ${}^3\text{H}$ – ${}^3\text{He}$  binding energy difference) to within roughly 30%. While at first sight this seems fine if one keeps in mind the expected uncertainty based on the EFT expansion, the relevant parameter in this case is actually not the  $Q/\Lambda_\pi$  of the strong sector (with the typical low-momentum scale set by the deuteron binding momentum,  $Q \sim \gamma_d \simeq 45$  MeV and the breakdown scale  $\Lambda_\pi \sim M_\pi \simeq 140$  MeV), but rather the  $\alpha M_N/Q$  scale (with  $M_N \simeq 940$  MeV) set by the Coulomb contributions. Since in the bound-state regime the momentum scale is set by the trinucleon binding momentum,  $\gamma_T \sim 80$  MeV, Coulomb effects are expected to be a small perturbation. Based on this, one should expect better agreement between perturbative and nonperturbative calculations.

The purpose of this work is to investigate a rearrangement of pionless EFT that explores the role of the increasing nuclear binding momentum in the simplest context, the trinucleon systems. We develop a new formulation to include Coulomb and other electromagnetic effects in nuclear ground states using perturbation theory. There are two important ingredients to this procedure. First, we introduce a new counting scheme that takes as LO the spin-singlet channel in the unitarity limit (infinite scattering length) and only includes the finite  ${}^1S_0$  scattering length as a perturbative correction. We will show with the  ${}^3\text{H}$  binding energy and with doublet  $nd$  scattering phase shifts that deviations from  ${}^1S_0$  unitarity are indeed small. In the case of  $pp$  scattering at very low energies, the scattering-length term is iterated along with Coulomb effects so that renormalization can be carried out by matching to the Coulomb-modified effective-range expansion. This is essentially what was introduced in Ref. [39], but here we isolate the contribution from the divergent single-photon bubble, which was missed in the perturbative calculation of Ref. [54]. This new scheme is the second ingredient which then allows us to use the counterterm fixed by  $pp$  scattering also in the perturbative calculation of the  ${}^3\text{H}$ – ${}^3\text{He}$  binding energy difference at next-to-leading order (NLO) in the new counting. The result differs from that of the nonperturbative calculation by much less than the 30% previously obtained, and is slightly closer to the experimental value of the binding energy difference. At NLO we end up about 1.5% off the  ${}^3\text{He}$  binding energy.

Besides finally obtaining a complete calculation of the energy splitting that includes Coulomb effects only as perturbative corrections, we also employ a fully perturbative treatment of corrections in the strong sector. This was already done in Ref. [26], which showed that a new, isospin-breaking three-body counterterm is needed for renormalization in the presence of range corrections when two-body Coulomb effects are resummed to all orders. A further motivation for the current paper is to revisit this issue with a completely perturbative

inclusion of those contributions as well.<sup>1</sup>

This paper is structured as follows. In Sec. II we discuss the basic formalism of pionless EFT with explicit isospin breaking. The two-body sector and in particular our new method to treat the  $pp$  channel is described in detail in Sec. III. In Sec. IV we discuss the implications for the three-body sector. The new results for the  ${}^3\text{H}$  and  ${}^3\text{He}$  binding energies are presented in Sec. V. We conclude in Sec. VI and provide technical details about the divergent Coulomb-bubble diagram in the Appendix.

## II. EFFECTIVE LAGRANGIAN

We are interested in describing nuclear bound states in terms of the most general dynamics consistent with QCD symmetries built from a nucleon field  $N$  of mass  $M_N$ . We use a modified and extended version of the notation and conventions in Refs. [52, 54]. To NLO we write the Lagrangian as

$$\mathcal{L} = N^\dagger \left( iD_0 + \frac{\mathbf{D}^2}{2M_N} \right) N + \mathcal{L}_{2d} + \mathcal{L}_{2t} + \mathcal{L}_3, \quad (1)$$

where  $D_\mu = \partial_\mu + ieA_\mu \hat{Q}_N$  includes the direct nucleon coupling to the electromagnetic field via the charge operator  $\hat{Q}_N = (1 + \tau_3)/2$ .

It is convenient to express the interaction terms via auxiliary dibaryon fields  $d^i$  and  $t^A$  in the  $NN$  channels projected with

$$P_d^i = \sigma^2 \sigma^i \tau^2 / \sqrt{8}, \quad P_t^A = \sigma^2 \tau^2 \tau^A / \sqrt{8}, \quad (2)$$

respectively, where lowercase (uppercase) letters are spin-1 (isospin-1) indices. While  $\hat{Q}_N$  ensures that Coulomb photons couple only to protons, the isospin-1 basis used for the spin-singlet field  $t^A$  otherwise mixes contributions from protons and neutrons. If we take  $A = 1, 2, 3$  to be an index in the Cartesian basis, then the  $np$  configurations are completely contained in the  $A = 3$  component, whereas  $nn$  and  $pp$  are obtained from linear combinations  $1 \pm i2$ . This corresponds to using a spherical basis  $\tilde{A} = -1, 0, 1$ , where one would immediately have the desired separation. We thus define new projectors

$$\tilde{P}_t^{-1} = \frac{1}{\sqrt{2}} (P_t^1 - iP_t^2), \quad \tilde{P}_t^0 = P_t^3, \quad \tilde{P}_t^{+1} = -\frac{1}{\sqrt{2}} (P_t^1 + iP_t^2) \quad (3)$$

that correspond to  $pp$ ,  $np$  and  $nn$  configurations, respectively. Since the transformation from  $P_t^A$  to  $\tilde{P}_t^{\tilde{A}}$  is a unitary rotation, the normalization is automatically correct:

$$\text{Tr} \left( (\tilde{P}_t^{\tilde{A}})^\dagger \tilde{P}_t^{\tilde{B}} \right) = \frac{1}{2} \delta_{\tilde{A}\tilde{B}}. \quad (4)$$

In terms of these fields and projectors, the two-body interactions are

$$\mathcal{L}_{2d} = -d^{i\dagger} \left[ \sigma_d + c_d \left( iD_0 + \frac{\mathbf{D}^2}{4M_N} \right) \right] d^i + y_d \left[ d^{i\dagger} (N^T P_d^i N) + \text{h.c.} \right] \quad (5)$$

---

<sup>1</sup> The viability of perturbative Coulomb exchange for the trinucleon system was also investigated in independent work [55], which appeared shortly after submission of our manuscript.

and

$$\begin{aligned} \mathcal{L}_{2t} = & -t^{0\dagger} \left[ \sigma_t + c_t \left( iD_0 + \frac{\mathbf{D}^2}{4M_N} \right) \right] t^0 - t^{-1\dagger} \left[ \sigma_{t,pp} + c_{t,pp} \left( iD_0 + \frac{\mathbf{D}^2}{4M_N} \right) \right] t^{-1} \\ & - t^{+1\dagger} \left[ \sigma_{t,nn} + c_{t,nn} \left( iD_0 + \frac{\mathbf{D}^2}{4M_N} \right) \right] t^{+1} + y_t \left[ t^{\tilde{A}\dagger} \left( N^T \tilde{P}_t^{\tilde{A}} N \right) + \text{h.c.} \right]. \end{aligned} \quad (6)$$

The covariant derivatives include the appropriate charge operators  $\hat{Q}$ . To keep the notation as simple as possible, we use the plain subscript “ $t$ ” to refer to the  $np$  channel from here on and use further qualifications only to denote  $pp$  and  $nn$  (the latter is not explicitly considered in the rest of this paper, except at the end of Sec. V). The parameters  $\sigma_d$  and  $\sigma_{t(\cdot\cdot)}$  are related to the respective scattering lengths; each is actually a sum of contributions from various orders:

$$\sigma_d = \sigma_d^{(0)} + \sigma_d^{(1)} + \cdots, \quad (7)$$

$$\sigma_{t(\cdot\cdot)} = \sigma_t^{(0)} + \sigma_{t(\cdot\cdot)}^{(1)} + \cdots. \quad (8)$$

A more detailed discussion is given in Ref. [54]. Departing from what is used there we follow here Ref. [56] and simply set

$$y_d^2 = y_t^2 = \frac{4\pi}{M_N}. \quad (9)$$

At the same time, the new parameters  $c_d$  and  $c_{t(\cdot\cdot)}$  have been introduced to incorporate effective-range corrections, *cf.* Fig. 2, starting at NLO:

$$c_d = c_d^{(1)} + \cdots, \quad (10)$$

$$c_{t(\cdot\cdot)} = c_t^{(1)} + \cdots. \quad (11)$$

In writing Eqs. (8) and (11) we imposed isospin symmetry at the lowest order of each parameter. The reason is that isospin violation comes from either electromagnetism or the up-down quark mass splitting. These are associated with mass scales  $\alpha M_N \sim 7$  MeV and  $m_u - m_d \sim 3$  MeV that are small compared to the breakdown scale  $\Lambda_{\pi}$ .

The three-nucleon interaction that is needed already at LO to renormalize the doublet-channel amplitude [14] can be written as [49, 57]

$$\mathcal{L}_3 = \frac{h}{3} N^\dagger \left[ y_d^2 d^{i\dagger} d^j \sigma^i \sigma^j + y_t^2 t^{A\dagger} t^B \tau^A \tau^B - y_d y_t (d^{i\dagger} t^A \sigma^i \tau^A + \text{h.c.}) \right] N, \quad (12)$$

where the coupling  $h$  is also split up in various orders,

$$h = h^{(0)} + h^{(1)} + \cdots. \quad (13)$$

As we are going to show below, there is no need for an isospin-breaking three-body force to NLO in our expansion. Higher-order terms, including further isospin violation, are briefly discussed in Sec. V.

### III. TWO-BODY SECTOR

In this section we use the Lagrangian from the previous section to derive the two-body propagators and amplitudes which are basic ingredients of the three-body calculation described in the next section.

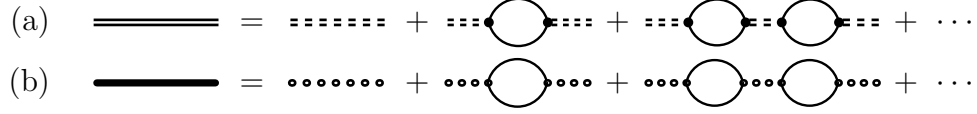


Figure 1: Full dibaryon propagators in (a) the  $^3S_1$  state (*i.e.*, the deuteron) and (b) the  $^1S_0$  state. A single solid line represents the propagation of a nucleon, a double dashed line a bare  $d$  propagator, and a line of circles a bare  $t$  propagator.

### A. Spin-triplet propagator

The dibaryon residual mass  $\sigma_d$  represents the physics of the triplet  $NN$  scattering length or, alternatively, the deuteron binding momentum  $\gamma_d$ . For momenta  $Q \sim \gamma_d \ll \Lambda_\pi$ , the standard power counting of pionless EFT applies [4, 5, 7, 9]. The bare LO dibaryon propagator is simply  $-i/\sigma_d^{(0)}$ , and it has to be dressed by nucleon bubbles to all orders in order to get the full LO expression. Summing up the geometric series shown diagrammatically in Fig. 1(a) gives

$$i\Delta_d^{(0)}(p_0, \mathbf{p}) = \frac{-i}{\sigma_d^{(0)} + y_d^2 I_0(p_0, \mathbf{p})}, \quad (14)$$

with the bubble integral

$$\begin{aligned} I_0(p_0, \mathbf{p}) &= M_N \int^\Lambda \frac{d^3 q}{(2\pi)^3} \frac{1}{M_N p_0 - \mathbf{p}^2/4 - \mathbf{q}^2 + i\varepsilon} \\ &= -\frac{M_N}{4\pi} \left( \frac{2\Lambda}{\pi} - \sqrt{\frac{\mathbf{p}^2}{4} - M_N p_0 - i\varepsilon} \right) + \mathcal{O}(1/\Lambda). \end{aligned} \quad (15)$$

Here, we have used a simple momentum cutoff  $\Lambda$  for regularization (not to be confused with the physical scale  $\Lambda_\pi$  at which pionless EFT breaks down because new dynamical degrees of freedom are resolved). To get expressions in the more commonly used power divergence subtraction (PDS) scheme [5], one has to replace  $2\Lambda/\pi \rightarrow \mu$ , where  $\mu$  is a scale introduced through dimensional regularization. Of course, in a properly renormalized theory the choice of regulator is arbitrary. While power counting is clean and transparent in the PDS scheme, we find it convenient here to work with the simple cutoff instead, because this regulator is more straightforward when it comes to the consistent treatment of Coulomb contributions. For completeness we note that Eq. (15) is valid up to corrections proportional to inverse powers of the cutoff, which we neglect here.

Range corrections are accounted for by the dibaryon kinetic parameter  $c_d$ , which is included fully perturbatively here. At NLO, we consider one insertion of the operator shown in Fig. 2(a) between  $\Delta_d^{(0)}$ s. Depending on the renormalization procedure, the insertion of  $c_d^{(1)}$  might require a concomitant insertion of  $\sigma_d^{(1)}$ ,

$$i\Delta_d^{(1)}(p_0, \mathbf{p}) = i\Delta_d^{(0)}(p_0, \mathbf{p}) \times \left[ -i\sigma_d^{(1)} - ic_d^{(1)} \left( p_0 - \frac{\mathbf{p}^2}{4M_N} \right) \right] \times i\Delta_d^{(0)}(p_0, \mathbf{p}). \quad (16)$$

In the spin-triplet channel, we use the effective range expansion around the deuteron pole for renormalization and thus require that

$$-iT(k) = (iy_d)^2 i\Delta_d(p_0 = k^2/M_N, \mathbf{p} = \mathbf{0}) = i \frac{4\pi}{M_N} \frac{1}{k \cot \delta_d(k) - ik}, \quad (17)$$

$$\begin{array}{cc}
\text{---}\times\text{---} \sim (-ic_d) \left( p_0 - \frac{\mathbf{p}^2}{4M_N} \right) & \text{---}\times\text{---} \sim (-ic_t) \left( p_0 - \frac{\mathbf{p}^2}{4M_N} \right) \\
\text{(a)} & \text{(b)}
\end{array}$$

Figure 2: Dibaryon kinetic-energy corrections in (a) the  $^3S_1$  state and (b) the  $^1S_0$  state.

with the perturbative expansion

$$\frac{1}{k \cot \delta_d(k) - ik} = \frac{1}{-\gamma_d + \frac{\rho_d}{2} (k^2 + \gamma_d^2) + \dots - ik} = \frac{1}{-\gamma_d - ik} \left[ 1 + \frac{\rho_d}{2} \frac{k^2 + \gamma_d^2}{\gamma_d + ik} + \dots \right], \quad (18)$$

where  $\gamma_d = \sqrt{M_N E_d} \simeq 45.7$  MeV [58] is the deuteron binding momentum and  $\rho_d \simeq 1.765$  fm [59] the deuteron effective range.

At LO, the effective range  $\rho_d \sim 1/\Lambda_{\pi}$  does not contribute and one simply has

$$\sigma_d^{(0)} = \frac{2\Lambda}{\pi} - \gamma_d. \quad (19)$$

The corresponding propagator  $\Delta_d^{(0)}$  is given by the term outside the parentheses in Eq. (18), up to an additional minus sign.

The corrections in the parentheses come from subleading orders. The first of these are  $\mathcal{O}(Q/\Lambda_{\pi}, \gamma_d/\Lambda_{\pi})$ , or NLO, and

$$\sigma_d^{(1)} = \frac{\rho_d \gamma_d^2}{2}, \quad c_d^{(1)} = \frac{M_N \rho_d}{2}. \quad (20)$$

## B. Spin-singlet propagators

In the spin-singlet channel, in the absence of Coulomb effects, we can follow the same procedure as in the spin-triplet channel (see Figs. 1(b) and 2(b)), and arrive at the LO propagator

$$i\Delta_t^{(0)}(p_0, \mathbf{p}) = \frac{-i}{\sigma_t^{(0)} + y_t^2 I_0(p_0, \mathbf{p})}. \quad (21)$$

At NLO, we have

$$i\Delta_t^{(1)}(p_0, \mathbf{p}) = i\Delta_t^{(0)}(p_0, \mathbf{p}) \times \left[ -i\sigma_t^{(1)} - ic_t^{(1)} \left( p_0 - \frac{\mathbf{p}^2}{4M_N} \right) \right] \times i\Delta_t^{(0)}(p_0, \mathbf{p}). \quad (22)$$

Renormalization is then performed by matching  $\Delta_t$  to the  $^1S_0$  effective range expansion around zero momentum,

$$k \cot \delta_t(k) = -\frac{1}{a_t} + \frac{r_t}{2} k^2 + \mathcal{O}(k^4), \quad (23)$$

where  $a_t \simeq -23.7$  fm and  $r_t \approx 2.73$  fm [60] are the  $np$  scattering length and effective range, respectively. As for the triplet,  $r_t \sim 1/\Lambda_{\pi}$ , but  $|a_t| \gg 1/\gamma_d$ .

### 1. Standard approach

Typically, one is interested in low momenta  $Q \sim 1/|a_t| \ll \Lambda_\pi$  and demands that at leading order the scattering length is reproduced. Effective-range and higher corrections are included perturbatively, since they are  $\mathcal{O}(Q/\Lambda_\pi, 1/(|a_t|\Lambda_\pi))$ . Up to NLO in this *standard* scheme one sets

$$\sigma_t^{(0,\text{st})} = \frac{2\Lambda}{\pi} - \frac{1}{a_t} \quad , \quad \sigma_t^{(1,\text{st})} = 0 \quad , \quad c_t^{(1,\text{st})} = \frac{M_N r_t}{2} . \quad (24)$$

There is no adjustment of  $\sigma_t$  when the effective-range expansion is performed around the zero-energy threshold.

### 2. Unitarity limit

The standard approach makes sense for momenta  $Q \sim 1/|a_t|$ , so at LO we have contributions from both the unitarity cut and the scattering length. However, if we are interested in momenta  $1/|a_t| \ll Q \ll \Lambda_\pi$ , we are close to the unitarity limit and take instead

$$\sigma_t^{(0)} = \frac{2\Lambda}{\pi} \quad , \quad \sigma_t^{(1)} = -\frac{1}{a_t} \quad , \quad c_t^{(1)} = \frac{M_N r_t}{2} , \quad (25)$$

so the actual finiteness of the scattering length only enters as a perturbative correction. The difference with respect to Eq. (24) is a result of  $|a_t| \gg 1/\gamma_d$ . For example, for  $Q \sim \gamma_d$ , we are performing an extra expansion in the ratio  $1/(|a_t|\gamma_d) \ll 1$ . Meanwhile, other effective range parameters require no special treatment, being similar in both channels—for example,  $r_t \sim \rho_d$ .

Of course, to the extent that this expansion works one might as well resum  $\sigma_t^{(1)}$  and use Eq. (24) with  $\sigma_t^{(0,\text{st})} = \sigma_t^{(0)} + \sigma_t^{(1)}$  over the whole range  $Q \ll \Lambda_\pi$ . However, there are also advantages in keeping a strict ordering. It makes clear, for example, that the singlet LO is parameter free. Also, as we show shortly, it matches well with the perturbative expansion of electromagnetic effects.

## C. Coulomb insertions

Simple dimensional analysis shows that the Coulomb expansion is in powers of  $\alpha M_N/Q$ , while other electromagnetic corrections are suppressed by at least  $(Q/\Lambda_\pi)^2$ . To NLO we need only keep the contribution from static Coulomb photons. In this case, the matching discussed above is correct for the  $np$  part of the  $^1S_0$  dibaryon. If one neglects strong isospin breaking, it can also be used to describe the  $nn$  component. For  $pp$  configurations, however, one has to use the Coulomb-modified effective range expansion [1, 39],

$$C_\eta^2 (k \cot \delta_{t,pp}(k) - ik) + \alpha M_N H(\eta) = -\frac{1}{a_C} + \frac{r_C}{2} k^2 + \dots \quad (26)$$

because electromagnetic effects dominate the very-low-energy scattering regime,  $Q \lesssim \alpha M_N$ . These are encoded in the Coulomb parameter

$$\eta(k) = \frac{\alpha M_N}{2k} , \quad (27)$$



the Gamow factor

$$C_\eta^2 = \frac{2\pi\eta}{e^{2\pi\eta} - 1}, \quad (28)$$

and the function

$$H(\eta) = \psi(i\eta) + \frac{1}{2i\eta} - \log(i\eta), \quad (29)$$

with  $\psi$  the derivative of the Euler Gamma function. Here  $a_C \simeq -7.81$  fm and  $r_C \simeq 2.79$  fm [61] are the Coulomb-modified scattering length and effective range, respectively. One arrives at Eq. (26) after subtracting the pure Coulomb amplitude with Coulomb phase shifts

$$\exp(2i\sigma_0) = \Gamma(1 + i\eta)/\Gamma(1 - i\eta) \quad (30)$$

from the full amplitude.

### 1. Kong+Ravndal approach

Since  $\alpha M_N \sim 1/|a_t|$ , describing physics at the scale of the  $^1S_0$  virtual state requires also a resummation of Coulomb exchange. This has been studied in detail by Kong and Ravndal in Ref. [39] in a setup without dibaryon fields. We refer to that reference for details and note here that the relation of our parameter  $\sigma_{t,pp}^{(0,st)}$  to the  $C_0$  of Kong and Ravndal is  $\sigma_{t,pp}^{(0,st)} = -4\pi/(M_N C_0)$ .

The key ingredient is the fully dressed Coulomb bubble shown in Fig. 3. From an evaluation of the Coulomb Green's function, Kong and Ravndal find that it is given by the divergent bubble integral

$$J_0(k) = M_N \int \frac{d^3q}{(2\pi)^3} \frac{2\pi\eta(q)}{e^{2\pi\eta(q)} - 1} \frac{1}{k^2 - q^2 + i\varepsilon}, \quad (31)$$

and they separate the divergent part with a subtraction at  $k = 0$ :

$$\begin{aligned} J_0(k) &= M_N \int \frac{d^3q}{(2\pi)^3} \frac{2\pi\eta(q)}{e^{2\pi\eta(q)} - 1} \frac{k^2}{q^2(k^2 - q^2 + i\varepsilon)} - M_N \int \frac{d^3q}{(2\pi)^3} \frac{2\pi\eta(q)}{e^{2\pi\eta(q)} - 1} \frac{1}{q^2} \\ &\equiv J_0^{\text{fin}}(k) + J_0^{\text{div}}, \end{aligned} \quad (32)$$

where the finite piece is

$$J_0^{\text{fin}}(k) = -\frac{\alpha M_N^2}{4\pi} H(\eta). \quad (33)$$

With a simple momentum cutoff, the divergent part is

$$J_0^{\text{div}} = -\frac{M_N \Lambda}{2\pi^2} + \frac{\alpha M_N^2}{4\pi} \left( \log \frac{2\Lambda}{\alpha M_N} - C_E \right) + \mathcal{O}(1/\Lambda), \quad (34)$$

where  $C_E \approx 0.5772$  is the Euler–Mascheroni constant, and we neglect higher-order corrections in  $1/\Lambda$ .

Resumming now this dressed bubble along with  $\sigma_{t,pp}^{(0,st)}$ , the singlet dibaryon propagator in the  $pp$  channel becomes

$$i\Delta_{t,pp}^{(0,st)}(p_0, \mathbf{p}) = \frac{-i}{\sigma_{t,pp}^{(0,st)} - \frac{2\Lambda}{\pi} + \alpha M_N \left( \log \frac{2\Lambda}{\alpha M_N} - C_E \right) - \alpha M_N H(\eta)}, \quad (35)$$

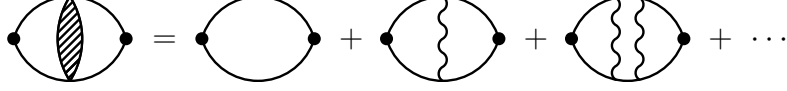


Figure 3: Fully dressed proton-proton bubble. A wavy line denotes a Coulomb photon exchange.

with

$$\eta = \eta \left( i \sqrt{\mathbf{p}^2/4 - M_N p_0 - i\epsilon} \right). \quad (36)$$

Matching to the Coulomb-modified effective range expansion is performed via the part of the T-matrix where Coulomb interferes with the short-range interactions,

$$-iT_{SC}(k) = C_\eta^2 e^{2i\sigma_0} (iy_t)^2 i\Delta_{t,pp}(p_0 = k^2/M_N, \mathbf{p} = \mathbf{0}) = i \frac{4\pi}{M_N} \frac{e^{2i\sigma_0}}{k \cot \delta_{t,pp}(k) - ik}. \quad (37)$$

The additional factors here compared to the  $np$  component, Eq. (17), arise from the inclusion of initial and final-state Coulomb interactions in order to get the amplitude from the propagator. Combining this relation with Eq. (26) one finds that both the Gamow factor and the pure Coulomb phase shift drop out and one arrives at

$$\sigma_{t,pp}^{(0,st)} = -\frac{1}{a_C} + \frac{2\Lambda}{\pi} - \alpha M_N \left( \log \frac{2\Lambda}{\alpha M_N} - C_E \right). \quad (38)$$

Range corrections were also considered in Ref. [39].

## 2. Separate leading-order resummation

Here we develop a new approach that allows us to consider a fully isospin-symmetric leading order in the spin-singlet channel, including the  $pp$  part. Since  $a_C$  is still large compared to the typical nuclear length scale set by the inverse pion mass ( $1/m_\pi \sim 1.4$  fm), in the momentum window  $\alpha M_N \lesssim 1/a_C \ll Q \ll \Lambda_\pi$  we remain close to unitarity in the singlet channels. We should be able to treat Coulomb perturbatively along with finite scattering-length corrections. The key idea is that with the new counting, the LO singlet propagator now behaves exactly like  $1/k$ , *i.e.*, it has the same infrared behavior as Coulomb contributions, for which the relevant parameter (in the  $pp$  system) is  $\eta = \alpha M_N/(2k)$ .

At LO we thus have, with an isospin-symmetric  $\sigma_t^{(0)}$  satisfying Eq. (25),

$$i\Delta_{t,pp}^{(0)}(p_0, \mathbf{p}) = i\Delta_t^{(0)}(p_0, \mathbf{p}) = \frac{-i}{\sqrt{\mathbf{p}^2/4 - M_N p_0 - i\epsilon}}. \quad (39)$$

At NLO, we need perturbative insertions not only of  $\sigma_{t,pp}^{(1)}$  (Fig. 4(a)) and  $c_t^{(1)}$  (Fig. 2(b)), but also of a single-photon exchange, see Fig. 4(b). Using the notation of Ref. [39], we call the single-photon piece  $\delta I_0(k)$  and find for the correction to the  $pp$  propagator:

$$i\Delta_{t,pp}^{(1)}(p_0, \mathbf{p}) = i\Delta_{t,pp}^{(0)}(p_0, \mathbf{p}) \times \left[ -i\sigma_{t,pp}^{(1)} - ic_t^{(1)} \left( p_0 - \frac{\mathbf{p}^2}{4M_N} \right) - iy_t^2 \delta I_0 \left( i \sqrt{\mathbf{p}^2/4 - M_N p_0 - i\epsilon} \right) \right] \times i\Delta_{t,pp}^{(0)}(p_0, \mathbf{p}). \quad (40)$$

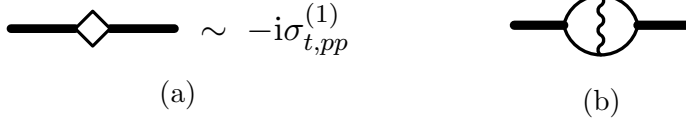


Figure 4: Corrections in the  $pp$  channel: (a) Coulomb-corrected scattering length; (b) one-photon exchange.

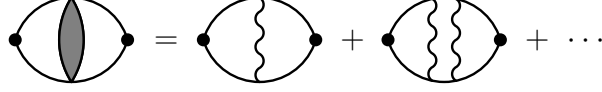


Figure 5: Dressed proton-proton bubble excluding the empty piece.

In order to match to the Coulomb-modified effective range expansion, we work in the  $pp$  center-of-mass frame in the remainder of this section. From the expression for  $\delta I_0(k)$  in Appendix A 1, we find for  $p_0 = k^2/M_N$ ,  $\mathbf{p} = \mathbf{0}$ , and  $\eta$  as defined in Eq. (27) that

$$\delta I_0(k) = \frac{\alpha M_N^2}{4\pi} \left[ \log i\eta + \log \frac{2\Lambda}{\alpha M_N} - C_\zeta \right] + \mathcal{O}(1/\Lambda), \quad (41)$$

where  $C_\zeta \simeq 1.119$  and we again drop terms proportional to inverse powers of  $\Lambda$ . The log divergence is absorbed into  $\sigma_{t,pp}^{(1)}$ , whereas the  $\log(i\eta)$  constitutes the one-photon contribution to  $H(\eta)$  as defined in Eq. (29).

In order to find the renormalization condition for  $\sigma_{t,pp}^{(1)}$ , we now consider smaller  $Q$ , which requires the resummation of both  $\sigma_{t,pp}^{(1)}$  and Coulomb exchange. We determine  $\sigma_{t,pp}^{(1)}$  from this calculation, and then use it in the regime where Coulomb is perturbative, to order  $\alpha$ . For this, it is important to be consistent about which finite terms get absorbed into  $\sigma_{t,pp}^{(1)}$  along with the logarithmic divergence.

The resummation of Coulomb produces a new dressed bubble, shown in Fig. 5. The important point is that this new dressed bubble excludes the empty piece (no photon exchange inside the bubble) because that has already been resummed at LO. We denote by  $\delta J_0(k)$  the part remaining after subtracting the single-photon piece  $\delta I_0(k)$ . In Appendix A 4 it is demonstrated that

$$\delta J_0(k) = -\frac{\alpha M_N^2}{4\pi} \left[ \psi(i\eta) + \frac{1}{2i\eta} + C_\Delta \right] + \frac{M_N}{4\pi} ik, \quad (42)$$

where  $C_\Delta \approx 0.579$ . Hence, we find for the new dressed bubble

$$\delta I_0(k) + \delta J_0(k) = \frac{\alpha M_N^2}{4\pi} \left[ \log \frac{2\Lambda}{\alpha M_N} - C_\zeta - C_\Delta - H(\eta) \right] + \frac{M_N}{4\pi} ik. \quad (43)$$

The resummation of  $\sigma_{t,pp}^{(1)}$  and the new dressed bubble is now straightforward. We consider here explicitly the on-shell case in the center-of-mass frame— $p_0 = k^2/M_N$ ,  $\mathbf{p} = \mathbf{0}$ —and find

$$\begin{aligned} i\Delta_{t,pp}^{\text{res}}(k) &= i\Delta_{t,pp}^{(0)}(k) + i\Delta_{t,pp}^{(0)}(k) \left( -i\sigma_{t,pp}^{(1)} - iy_t^2 \delta I_0(k) - iy_t^2 \delta J_0(k) \right) i\Delta_{t,pp}^{(0)}(k) + \dots \\ &= \frac{-i}{\underbrace{\sigma_t^{(0)} - \frac{2\Lambda}{\pi}}_{=0} + \sigma_{t,pp}^{(1)} + \alpha M_N \left( \log \frac{2\Lambda}{\alpha M_N} - C_\zeta - C_\Delta \right) - \alpha M_N H(\eta)}, \end{aligned} \quad (44)$$

where the explicit imaginary part  $ik$  cancels. Now, from Eqs. (37) and (26),

$$\sigma_{t,pp}^{(1)} = -\frac{1}{a_C} - \alpha M_N \left( \log \frac{2\Lambda}{\alpha M_N} - C_\zeta - C_\Delta \right), \quad (45)$$

Our renormalization of  $\sigma_{t,pp}^{(0)} + \sigma_{t,pp}^{(1)}$  is consistent with Eq. (38), but with a different constant finite piece. As discussed in more detail in the Appendix, the reason for this change is that we have isolated here the divergent piece—the bubble with a single photon exchange—and only regularized that, whereas Ref. [39] regularizes the fully resummed bubble—including the empty part—at once. Effectively, this amounts to using different regularization schemes. Our approach has the advantage that it allows for a consistent matching between the perturbative and nonperturbative regimes.

The expression for the  $pp$  phase shift in the regime  $\alpha M_N \lesssim 1/|a_C| \ll Q \ll \Lambda_\pi$  can now be found by inserting Eqs. (39) and (40) into Eq. (37):

$$k \cot \delta_{t,pp}(k) = -\frac{1}{a_C} + \alpha M_N C_\Delta + \frac{r_t}{2} k^2 + \alpha M_N \log \left( \frac{\alpha M_N}{2k} \right) + \dots. \quad (46)$$

This is consistent with a direct expansion of Eq. (26) in powers of  $\alpha M_N/Q$  and  $1/(|a_C|Q)$ . Using

$$\psi(i\eta) = \frac{i}{\eta} - C_E + \mathcal{O}(\eta), \quad (47)$$

one finds Eq. (46) with  $C_\Delta = C_E$  and

$$r_C^{\text{NLO}} = r_t. \quad (48)$$

Moreover, the same result as in Eq. (46) can be obtained in a direct calculation that includes all  $\mathcal{O}(\alpha)$  diagrams contributing to  $pp$  scattering, treated in perturbation theory.

As discussed in Appendix A 4, a numerical calculation indeed yields  $C_\Delta \approx 0.579$ , very close to  $C_E \approx 0.5772$ . Equation (46) gives circumstantial evidence that in fact  $C_\Delta = C_E$ , and we expect that increased numerical accuracy would reveal the same. Lacking a formal proof, however, we keep  $C_\Delta$  in the expressions here and merely note that the deviation from  $C_E$  is negligible for the results presented later.

Equation (46) is in agreement with the Nijmegen phase-shift analysis [62] up to about 15% for  $k \gtrsim 60$  MeV. In particular, it captures the correct slope at intermediate momenta, which is a consequence of the fact that Eq. (48) works at the 3% level. The assumption of isospin symmetry in  $c_t^{(1)}$ , which means that we can neglect the splitting in the spin-singlet ranges, is a good one.

#### IV. THREE-BODY SECTOR

We now consider the three-body sector in order to calculate the  $^3\text{H}$  and  $^3\text{He}$  binding energies. These bound states arise in the  $nd$  and  $pd$  spin-doublet channels, respectively. Since we do not reorganize the pionless EFT expansion in the  $NN$  spin-triplet channel, no changes are needed in the  $nd$  and  $pd$  spin-quartet channels with respect to Refs. [3, 6, 11, 12, 24, 25].

We take the point of view that the scale that characterizes these bound states, the triton binding momentum  $\gamma_T$ , is comparable to the deuteron binding momentum  $\gamma_d$ , but both are

much larger than  $\alpha M_N$ ,  $1/|a_t|$ , and  $1/|a_C|$ . Thus the bound-state energies can be expanded not only in powers of  $Q/\Lambda_\pi$  but also of  $\aleph_0/Q$ , where  $\aleph_0 \sim \alpha M_N \sim 1/|a_t| \sim 1/|a_C|$ .<sup>2</sup> For simplicity we pair the two expansions by taking  $Q \sim (\aleph_0 \Lambda_\pi)^{1/2}$ .

### A. More formalism

According to the standard power counting [3, 6, 11, 12] one-nucleon exchange between nucleon and dibaryon has to be treated exactly. To NLO it is sufficient to consider the  $S$ -wave projected one-nucleon-exchange diagram at energy  $E$ ,

$$K_s(E; k, p) \equiv \frac{1}{kp} Q_0 \left( \frac{k^2 + p^2 - M_N E - i\varepsilon}{kp} \right) = \frac{1}{2kp} \log \left( \frac{k^2 + p^2 + kp - M_N E - i\varepsilon}{k^2 + p^2 - kp - M_N E - i\varepsilon} \right), \quad (49)$$

where  $k$  ( $p$ ) is the incoming (outgoing) center-of-mass momentum. It is well known [14–19] that at LO the resummation of one-nucleon exchange is renormalized by the three-body force given in Eq. (12), with

$$h^{(0)} = \frac{M_N H(\Lambda)}{\Lambda^2}, \quad (50)$$

where  $\Lambda$  is now the momentum cutoff applied in the three-body equations discussed below, and  $H(\Lambda)$  a known log-periodic function of the cutoff that depends on a three-body parameter  $\Lambda_*$ . Here we follow the procedure employed in Ref. [3] and much of the subsequent literature, in which the two-body cutoff is taken to be very large and  $\mathcal{O}(1/\Lambda)$  terms in Eqs. (15) and (41) are neglected.<sup>3</sup>

In order to calculate bound-state energies and perturbative corrections to them, we use the formalism and notation of Refs. [52, 54] to study the  $Nd$  doublet channel. We introduce a three-component vector of vertex functions in channel space,

$$\vec{\mathcal{B}}_s \equiv (\mathcal{B}_s^{\text{d,a}}, \mathcal{B}_s^{\text{d,b1}}, \mathcal{B}_s^{\text{d,b2}})^T, \quad (51)$$

where  $\mathcal{B}_s^{\text{d,a}}$  corresponds to the deuteron channel and  $\mathcal{B}_s^{\text{d,b1}}$  and  $\mathcal{B}_s^{\text{d,b2}}$  are the  $np$  and  $pp/nn$  components of the  $^1S_0$  multiplet, respectively. These are given by (properly normalized [47]) solutions of the homogeneous equation

$$\vec{\mathcal{B}}_s = (\hat{K} \hat{D}) \otimes \vec{\mathcal{B}}_s, \quad E = -E_B, \quad (52)$$

where  $\otimes$  represents an integral over the intermediate momentum,  $\hat{D}$  is a diagonal matrix of dibaryon propagators written in the form

$$D_{d,t}(E; q) = \Delta_{d,t} \left( E - \frac{q^2}{2M_N}; q \right), \quad (53)$$

<sup>2</sup> Note that  $\aleph_0$  is an extension of the original definition [4, 9] to include additional scales, in particular  $\alpha M_N$ .

<sup>3</sup> This is effectively equivalent to using dimensional regularization in order to renormalize the two-body sector first.

and

$$\hat{K} \equiv \begin{pmatrix} -g_{dd} \left( K_s + \frac{2H(\Lambda)}{\Lambda^2} \right) & g_{dt} \left( 3K_s + \frac{2H(\Lambda)}{\Lambda^2} \right) & g_{dt} \left( 3K_s + \frac{2H(\Lambda)}{\Lambda^2} \right) \\ g_{dt} \left( K_s + \frac{2H(\Lambda)}{3\Lambda^2} \right) & g_{tt} \left( K_s - \frac{2H(\Lambda)}{3\Lambda^2} \right) & -g_{tt} \left( K_s + \frac{2H(\Lambda)}{3\Lambda^2} \right) \\ g_{dt} \left( 2K_s + \frac{4H(\Lambda)}{3\Lambda^2} \right) & -g_{tt} \left( 2K_s + \frac{4H(\Lambda)}{3\Lambda^2} \right) & -g_{tt} \frac{4H(\Lambda)}{3\Lambda^2} \end{pmatrix}. \quad (54)$$

The factors  $g_{dd}$  *etc.* contain the coupling constants  $y_d$  and  $y_t$ . In our present conventions, we simply have

$$g_{dd} = g_{tt} = g_{dt} = 2\pi. \quad (55)$$

For illustration, we note that with a single channel and no three-body force, the homogeneous integral equation written out explicitly would be

$$\mathcal{B}_s(p) = \frac{1}{\pi} \int_0^\Lambda dq q^2 K_s(E; p, q) \Delta \left( E - \frac{q^2}{2M_N}; q \right) \mathcal{B}_s(q), \quad (56)$$

where  $\Delta$  denotes a generic dibaryon propagator, and  $\Lambda$  is the momentum cutoff employed in the three-body sector.

To study doublet-channel  $nd$  scattering, we have to solve the Lippmann–Schwinger equation. This can be done in a simpler two-channel formalism, where it becomes

$$\begin{pmatrix} \mathcal{T}_s^{\text{d,a}} \\ \mathcal{T}_s^{\text{d,b}} \end{pmatrix} = \begin{pmatrix} g_{dd} \left( K_s + \frac{2H(\Lambda)}{\Lambda^2} \right) \\ -g_{dt} \left( 3K_s + \frac{2H(\Lambda)}{\Lambda^2} \right) \end{pmatrix} + \begin{pmatrix} -g_{dd} D_d \left( K_s + \frac{2H(\Lambda)}{\Lambda^2} \right) & g_{dt} D_t \left( 3K_s + \frac{2H(\Lambda)}{\Lambda^2} \right) \\ g_{dt} D_d \left( 3K_s + \frac{2H(\Lambda)}{\Lambda^2} \right) & -g_{tt} D_t \left( K_s + \frac{2H(\Lambda)}{\Lambda^2} \right) \end{pmatrix} \otimes \begin{pmatrix} \mathcal{T}_s^{\text{d,a}} \\ \mathcal{T}_s^{\text{d,b}} \end{pmatrix}. \quad (57)$$

Again, the notation is the same as in Refs. [52, 54]. The  $nd$  phase shift is then obtained from the on-shell amplitude,

$$\delta_{n-d}(k) = \frac{1}{2i} \log \left( 1 + \frac{2ikM_N}{3\pi} Z_0 \mathcal{T}_s^{\text{d,a}}(E_k; k, k) \right), \quad E_k = \frac{3k^2}{4M_N} - \frac{\gamma_d^2}{M_N}, \quad (58)$$

where  $Z_0$  is the deuteron wavefunction renormalization determined by

$$Z_0^{-1} = i \frac{\partial}{\partial p_0} \frac{1}{\Delta_d(p)} \Big|_{p_0 = -\frac{\gamma_d^2}{M_N}, \mathbf{p}=0}. \quad (59)$$

The scattering length is determined by the on-shell amplitude in the limit  $k \rightarrow 0$ ,

$$^2a_{n-d} = -\frac{M_N}{3\pi} \lim_{k \rightarrow 0} Z_0 \mathcal{T}_s^{\text{d,a}}(E_k; k, k). \quad (60)$$

## B. Perturbative range corrections

Before we discuss Coulomb matrix elements between vertex functions, it is instructive to consider effective-range corrections in this framework. As we emphasized in Sec. III, range



Figure 6: Range corrections contributing to the trinucleon binding energy in perturbation theory. A shaded oval represents a vertex function.

corrections are  $\mathcal{O}(Q/\Lambda_\pi)$ . In analogy to Eq. (18), we write

$$D_d(E; q) = D_d^{(0)}(E; q) + D_d^{(1)}(E; q) + \dots$$

$$= \frac{-1}{-\gamma_d + \sqrt{3q^2/4 - M_N E - i\varepsilon}} \times \left[ 1 + \frac{\rho_d}{2} \frac{(3q^2/4 - M_N E - \gamma_d^2)}{-\gamma_d + \sqrt{3q^2/4 - M_N E - i\varepsilon}} + \dots \right], \quad (61)$$

with an analogous expression for the spin-singlet part. Suppose now we have solved the homogeneous equation (52) at leading order. The binding-energy shift due to the deuteron effective range, shown in Fig. 6(a), is then given by

$$\Delta E_{\rho_d}^{(1)} = \frac{\rho_d}{4\pi^2} \int_0^\Lambda dq q^2 |\mathcal{B}_s^{d,a}(q)|^2 \frac{(3q^2/4 - M_N E - \gamma_d^2)}{\left(-\gamma_d + \sqrt{3q^2/4 - M_N E - i\varepsilon}\right)^2}. \quad (62)$$

More details about this can be found in Refs. [24, 26]. In particular, we note that the correction  $h^{(1)}$  to the three-body force is fitted to keep whatever physical parameter has been used at LO (triton binding energy or doublet-channel scattering length) unchanged.

In the *standard* counting used previously (finite scattering lengths at LO), there is a contribution analogous to Eq. (62) with  $\gamma_d \rightarrow 1/a_t$  in the denominator (and no  $\gamma_d$  in the numerator). In our new scheme with the spin-singlet LO in the unitarity limit, the range corrections in the spin-singlet channels are particularly simple. For example, from Fig. 6(b) we have

$$\Delta E_{r_t, b1}^{(1)} = \frac{3r_t}{4\pi^2} \int_0^\Lambda dq q^2 |\mathcal{B}_s^{d,b1}(q)|^2, \quad (63)$$

and an analogous expression that involves  $\mathcal{B}_s^{d,b2}$ . NLO corrections that are linear in the range have been known for a long time to generate cutoff dependence that can be compensated by  $h^{(1)}$  [14, 16, 19]. For three bosons at unitarity, this divergence was discussed in Refs. [63, 64]. At the same time, we have of course now perturbative insertions of the scattering length, *e.g.*,

$$\Delta E_{a_t, b1}^{(1)} = \frac{3}{2\pi^2 a_t} \int_0^\Lambda dq q^2 \frac{|\mathcal{B}_s^{d,b1}(q)|^2}{3q^2/4 + M_N E_B}, \quad (64)$$

which are corrections of  $\mathcal{O}(\mathbb{N}_0/Q)$  relative to LO.

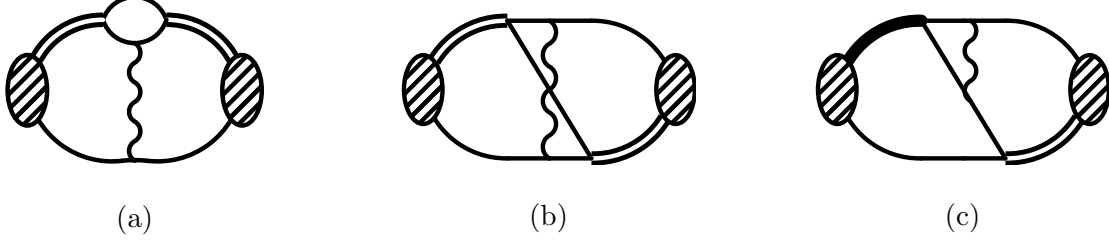


Figure 7: Convergent diagrams contributing to the  ${}^3\text{H}$ - ${}^3\text{He}$  binding energy difference in perturbation theory.



Figure 8: Divergent Coulomb bubble diagram (a) contributing to the  ${}^3\text{H}$ - ${}^3\text{He}$  binding energy difference along with the associated counterterm (b).

### C. Coulomb matrix elements

Range corrections as discussed in the previous section apply in general to both  $nd$  and  $pd$  systems. In the bound-state regime, they simply correspond to matrix elements between trinucleon wavefunctions that are diagonal in momentum space (only one loop integral is required to calculate them) as well as in cluster-configuration (channel) space [56].

Now we want to include Coulomb corrections, which are  $\mathcal{O}(\kappa_0/Q)$ . In general, contributions to the  ${}^3\text{H}$ - ${}^3\text{He}$  energy splitting  $\Delta E$  can be non-diagonal in both spaces. We get such contributions when we calculate  $\Delta E$  in perturbation theory, which comes from diagram topologies shown in Figs. 7 and 8. This approach starts by taking the trinucleon state to be the triton in a three-channel formalism. This way, one can easily isolate the channel that corresponds to the  $pp$  configuration in  ${}^3\text{He}$ . Such a calculation was carried out in Ref. [54] for the diagrams in Fig. 7, which give convergent results. We briefly summarize this calculation here before getting to the new diagrams in Fig. 8.

The diagram shown in Fig. 7(a) is still diagonal in cluster-configuration space. In order to calculate it, we need the kernel function corresponding to the photon being exchanged between the deuteron bubble and the individual proton. It is given by [47]

$$K_{\text{bubble}}(E; k, p) = -\alpha M_N \int_{-1}^1 d\cos\theta \frac{\mathcal{I}_{\text{bubble}}(E; \mathbf{k}, \mathbf{p})}{(\mathbf{k} - \mathbf{p})^2 + \lambda^2} \quad , \quad \mathbf{k} \cdot \mathbf{p} = kp \cos\theta \quad , \quad (65)$$

with

$$\mathcal{I}_{\text{bubble}}(E; \mathbf{k}, \mathbf{p}) = \frac{\arctan\left(\frac{2\mathbf{p}^2 - \mathbf{k}^2 - \mathbf{k} \cdot \mathbf{p}}{\sqrt{3\mathbf{k}^2 - 4M_N E - i\epsilon}\sqrt{(\mathbf{k} - \mathbf{p})^2}}\right) + \arctan\left(\frac{2\mathbf{k}^2 - \mathbf{p}^2 - \mathbf{k} \cdot \mathbf{p}}{\sqrt{3\mathbf{p}^2 - 4M_N E - i\epsilon}\sqrt{(\mathbf{k} - \mathbf{p})^2}}\right)}{\sqrt{(\mathbf{k} - \mathbf{p})^2}} \quad , \quad (66)$$



and where  $\lambda$  is a photon mass introduced for regularization in the infrared. In practice, we do not perform the angular integral numerically but rather use the explicit  $S$ -wave projection given in Ref. [26]. The contribution to the energy shift is then given by

$$\Delta E_{7(a)}^{(1)} = \frac{1}{2\pi^3} \int_0^\Lambda dq_1 q_1^2 \int_0^\Lambda dq_2 q_2^2 \mathcal{B}_s^{\text{d},a}(q_1) D_d^{(0)}(-E_B, q_1) \\ \times K_{\text{bubble}}(E; q_1, q_2) D_d^{(0)}(-E_B, q_2) \mathcal{B}_s^{\text{d},a}(q_2). \quad (67)$$

The analogous diagram with  $np$  singlet propagators (not shown explicitly in Fig. 7) is given by essentially the same expression with the replacements  $\mathcal{B}_s^{\text{d},a} \rightarrow \mathcal{B}_s^{\text{d},b1}$  and  $D_d \rightarrow D_t$ . For the “box” and “triangle” contributions, Figs. 7(b) and (c), the corresponding kernel functions are [54]

$$K_{\text{box}}(E; k, p) = -\alpha M_N \\ \times \frac{1}{2} \int_{-1}^1 d\cos\theta \left\{ \frac{\arctan\left(\frac{2\mathbf{p}^2 - \mathbf{k}^2 - \mathbf{k} \cdot \mathbf{p}}{\sqrt{3\mathbf{k}^2 - 4M_N E - i\varepsilon} \sqrt{(\mathbf{k} - \mathbf{p})^2}}\right) + \arctan\left(\frac{2\mathbf{k}^2 - \mathbf{p}^2 - \mathbf{k} \cdot \mathbf{p}}{\sqrt{3\mathbf{p}^2 - 4M_N E - i\varepsilon} \sqrt{(\mathbf{k} - \mathbf{p})^2}}\right)}{(\mathbf{k}^2 + \mathbf{p}^2 + \mathbf{k} \cdot \mathbf{p} - M_N E - i\varepsilon) \sqrt{(\mathbf{k} - \mathbf{p})^2}} \right. \\ \left. - \frac{\lambda}{(\mathbf{k}^2 + \mathbf{p}^2 + \mathbf{k} \cdot \mathbf{p} - M_N E - i\varepsilon)^2} + \mathcal{O}(\lambda^2) \right\}, \quad (68)$$

and

$$K_{\text{tri}}^{(\text{out})}(E; k, p) = -\alpha M_N \times \frac{1}{2} \int_{-1}^1 d\cos\theta \frac{\mathcal{I}_{\text{tri}}(E; \mathbf{k}, \mathbf{p})}{\mathbf{k}^2 + \mathbf{p}^2 + \mathbf{k} \cdot \mathbf{p} - M_N E - i\varepsilon}, \quad (69a)$$

$$K_{\text{tri}}^{(\text{in})}(E; k, p) = K_{\text{tri}}^{(\text{out})}(E; p, k), \quad (69b)$$

where the superscripts “out” and “in” indicate whether the Coulomb-photon exchange is on the left or right side of the diagram. This notation is taken over from Ref. [54], which allowed for incoming and outgoing  $pd$  states. The loop function appearing in Eq. (69a) is given by

$$\mathcal{I}_{\text{tri}}(E; \mathbf{k}, \mathbf{p}) = \frac{i}{2\sqrt{\mathbf{k}^2/4 + \mathbf{k} \cdot \mathbf{p} + \mathbf{p}^2}} \\ \times \left\{ \log \left( \frac{i(\mathbf{k}^2/2 - \mathbf{k} \cdot \mathbf{p} - \mathbf{p}^2 - \lambda^2 - M_N E - i\varepsilon)}{\sqrt{\mathbf{k}^2/4 + \mathbf{k} \cdot \mathbf{p} + \mathbf{p}^2}} + 2\sqrt{\lambda^2 + 3\mathbf{k}^2/4 - M_N E - i\varepsilon} \right) \right. \\ \left. - \log \left( \frac{i(\mathbf{k}^2 + \mathbf{p}^2 + \mathbf{k} \cdot \mathbf{p} - \lambda^2 - M_N E - i\varepsilon)}{\sqrt{\mathbf{k}^2/4 + \mathbf{k} \cdot \mathbf{p} + \mathbf{p}^2}} + 2\lambda \right) \right\}. \quad (70)$$

As for  $K_{\text{bubble}}(E; k, p)$ , explicit  $S$ -wave projections where the integral over  $\cos\theta$  has been carried out analytically can be found in Ref. [26]. Resulting contributions to the energy shift are of the form

$$\Delta E_{7(b)}^{(1)} = \frac{1}{2\pi^3} \int_0^\Lambda dq_1 q_1^2 \int_0^\Lambda dq_2 q_2^2 \mathcal{B}_s^{\text{d},a}(q_1) D_d^{(0)}(-E_B, q_1) \\ \times K_{\text{box}}(E; q_1, q_2) D_d^{(0)}(-E_B, q_2) \mathcal{B}_s^{\text{d},a}(q_2) \quad (71)$$

and

$$\Delta E_{7(c)}^{(1)} = -\frac{3}{2\pi^3} \int_0^\Lambda dq_1 q_1^2 \int_0^\Lambda dq_2 q_2^2 \mathcal{B}_s^{\text{d},\text{b1}}(q_1) D_t^{(0)}(-E_B, q_1) \times K_{\text{tri}}^{(\text{out})}(E; q_1, q_2) D_d^{(0)}(-E_B, q_2) \mathcal{B}_s^{\text{d},\text{a}}(q_2), \quad (72)$$

with analogous expressions for equivalent topologies but different combinations of dibaryon propagators and vertex functions (see Ref. [54] for details).

The above summarizes the diagrams included in the perturbative calculation of Ref. [54]; all these contributions are convergent as the cutoff  $\Lambda$  is increased. As mentioned in the introduction, the contribution from the diagram shown in Fig. 8(a) has not been included so far. This diagram is logarithmically divergent, but this is precisely the same divergence of the one-photon bubble that we isolated in the new treatment of the two-body sector discussed in Sec. III C 2. Hence, it can be renormalized by including it together with the counterterm diagram shown in Fig. 8(b), which is proportional to  $\sigma_{t,pp}^{(1)}$  as given in Eq. (45). The resulting contribution to the energy shift, written out explicitly, is

$$\Delta E_{8(a+b)}^{(1)} = \frac{3}{4\pi^2} \int_0^\Lambda dq q^2 \frac{|\mathcal{B}_s^{\text{d},\text{b2}}(q)|^2}{3q^2/4 + M_N E_B} \times \left\{ \frac{1}{a_C} - \alpha M_N \left[ C_\Delta + \log \left( \frac{\alpha M_N}{2\sqrt{M_N E_B + 3q^2/4}} \right) \right] \right\}. \quad (73)$$

Note that the constant  $C_\zeta$  drops out here against the same contribution from the photon bubble, *cf.* Eq. (41). Expanding the *renormalized*  $pp$  propagator of Refs. [49, 54] in  $\alpha$  gives Eq. (73) with  $C_\Delta \rightarrow C_E$ , as expected from their similar values (*cf.* the discussion in Sec. III C 2).

We stress here that the new approach takes all spin-singlet propagators in the unitarity limit at LO. In the  $pp$  channel, the finite scattering length  $a_C$  is included together with the single-photon bubble contribution, resulting in Eq. (73). At the same time, we also include linear insertions of  $1/a_t$  in the  $np$  spin-singlet channel, as given in Eq. (64).

## V. RESULTS AND DISCUSSION

We summarize our new expansion as follows: at leading order, we include

- the standard  $NN$  spin-triplet (pionless) amplitude (parameter  $\gamma_d$ ),
- the unitary  $NN$  spin-singlet amplitude (parameter-free),
- a contact three-body force (parameter  $\Lambda_*$ ).

Our new NLO includes<sup>4</sup>

- the effective range in the  $NN$  spin-triplet channel (parameter  $\rho_d$ ),

<sup>4</sup> These NLO contributions induce corrections to the spin-triplet two- and three-body force parameters that already appeared at LO, but these corrections introduce no new parameters.

Parameter	Value	Ref.
$\gamma_d$	45.7 MeV	[58]
$\rho_d$	1.765 fm	[59]
$a_t$	-23.714 fm	[60]
$r_t$	2.73 fm	[60]
$a_C$	-7.8063 fm	[61]

Table I: Parameters used for the numerical calculation.

- the isospin-symmetric range in the  $NN$  spin-singlet channel (parameter  $r_t$ ),
- a scattering-length correction to unitarity in the  $NN$  spin-singlet  $np$  and  $nn$  channels (parameter  $a_t$ ),
- a scattering-length correction to unitarity in the  $NN$   $pp$  channel (parameter  $a_C$ ),
- one-photon exchange (parameter  $\alpha = 1/137$ ).

The two-body parameters we use in our numerical calculation are summarized in Table I. For the nucleon mass we take  $M_N = 938.918$  MeV.

Unitarity in the  $NN$  spin singlet at LO means that our results for the binding energies and scattering of nuclei differ from previous calculations, for example the  ${}^3\text{H}$  binding energy and  $nd$  scattering in the doublet channel [14–18]. In order to facilitate the comparison with existing, standard-LO results, we also consider below an “incomplete” new NLO, where we set  $\rho_d = r_t = 0$ .

In the spin singlet we perform an extra  $\aleph_0/Q$  expansion on top of the standard  $Q/\Lambda_\pi$  expansion. We first show that the  $\aleph_0/Q$  expansion gives results that are in good agreement with the standard leading-order  $NN$  spin-singlet amplitude in the absence of Coulomb effects. As  $\Lambda_*$  is varied with fixed  $NN$  input, doublet-channel observables change in a correlated way. The simplest example is the Phillips line [20] in the plane of  ${}^3\text{H}$  binding energy and  $nd$  scattering length, see Fig. 9. Five curves are shown for a three-body cutoff  $\Lambda = 2.4$  GeV; effects from further increasing the cutoff are negligible. In three of the curves the ranges are set to zero. We see that the new LO curve (with  $a_t \rightarrow \infty$ ) is within 1% of the standard LO curve (with  $a_t$  at its physical value), and the new LO+(incomplete)NLO (with  $a_t \rightarrow \infty$  at LO and  $1/a_t$  at its physical value treated in first-order perturbation theory, but zero range) is closer still. The inset magnifies a region of the plot to show the small differences among these curves. This agreement is not fortuitous and survives the inclusion of range corrections, displayed in the other two curves. Again, the new LO+NLO curve ( $a_t \rightarrow \infty$  at LO, and both physical  $1/a_t$  and ranges in first-order perturbation theory) is very close to the standard LO+NLO ( $a_t$  at its physical value at LO, ranges in first-order perturbation theory).

In Fig. 9 we also indicate the experimental values of the  ${}^3\text{H}$  binding energy and doublet  $nd$  scattering length by, respectively, horizontal and vertical lines. Leading-order curves (new as well as standard) lie close to the experimental point. Next-order curves (new as well as standard) are small shifts in the direction of data, overshooting a bit.

We can use either the binding energy or the doublet-channel scattering length to determine  $\Lambda_*$ , and then the other is a prediction that nearly agrees with data. Here we use the  ${}^3\text{H}$  binding energy,  $E_B({}^3\text{H}) = 8.48$  MeV, as input. At LO this is done by adjusting  $h^{(0)}$ ; at

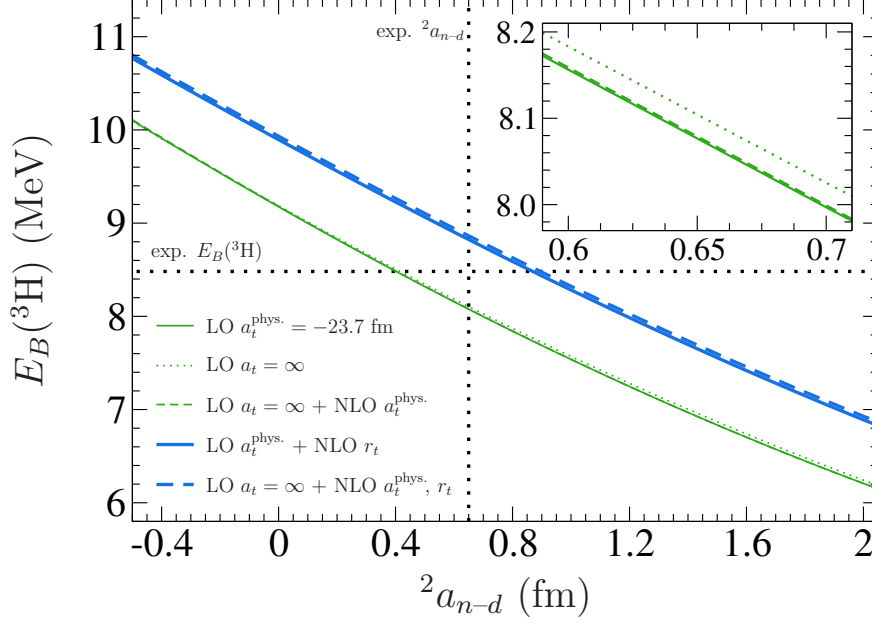


Figure 9: Correlation (Phillips line) between  ${}^3\text{H}$  binding energy (in MeV) and doublet  $nd$  scattering length (in fm) at LO and NLO. The light (green) and dark (blue) solid lines are the results of the standard expansion at LO and LO+NLO. The light (green) dotted line is the new LO, the light (green) dashed line is the new LO+NLO with ranges set to zero, and the dark (blue) dashed line is the full new LO+NLO. All curves are for a three-body cutoff  $\Lambda = 2.4$  GeV. Horizontal and vertical (black) dotted lines indicate experimental values for binding energy and scattering length, respectively.

NLO,  $h^{(1)}$  ensures that the  ${}^3\text{H}$  binding energy remains at its experimental value. The same procedure is used in the standard expansion with  $a_t$  in the LO propagators, and our values for  $h^{(0,1)}$  come out very close to results in that approach [26]. Then the  $nd$  scattering length converges as the cutoff  $\Lambda$  increases, as shown in Fig. 10, where five curves analogous to those in Fig. 9 are displayed. More generally, Fig. 11 shows the predictions for the doublet-channel  $nd$  phase shifts at low momenta. Again, the effects of treating the finite value of the singlet scattering length in perturbation theory are small.

Thus, the  $\aleph_0/Q$  expansion works quite well in the absence of Coulomb interactions. In fact, range corrections seem larger than those from the finite singlet scattering length, which suggests that the  $\aleph_0/Q$  expansion works better than the  $Q/\Lambda_\pi$  expansion. With the  ${}^3\text{H}$  channel properly renormalized and the three-body force fixed, we now consider Coulomb corrections to the  ${}^3\text{He}$  binding energy. Because our LO Lagrangian is isospin-symmetric, the  ${}^3\text{H}$ – ${}^3\text{He}$  binding energy difference vanishes in our new LO, but it is a prediction—a low-energy theorem—at NLO.

To gauge the effects of perturbative Coulomb corrections, we show in Fig. 12 the result of the new calculation presented here at NLO, as a function of the cutoff. The photon mass  $\lambda$  has been extrapolated to zero in the same way as in Ref. [54], that is, a linear extrapolation based on the range  $\lambda = 0.4 \dots 0.6$  MeV. All Coulomb effects, including those in the  $pp$  sector, are included fully perturbatively here, meaning that we only consider matrix elements between trinucleon wavefunctions that involve a single Coulomb-photon exchange. We find that the inclusion of the renormalized Coulomb-bubble diagram, Fig. 8, ensures

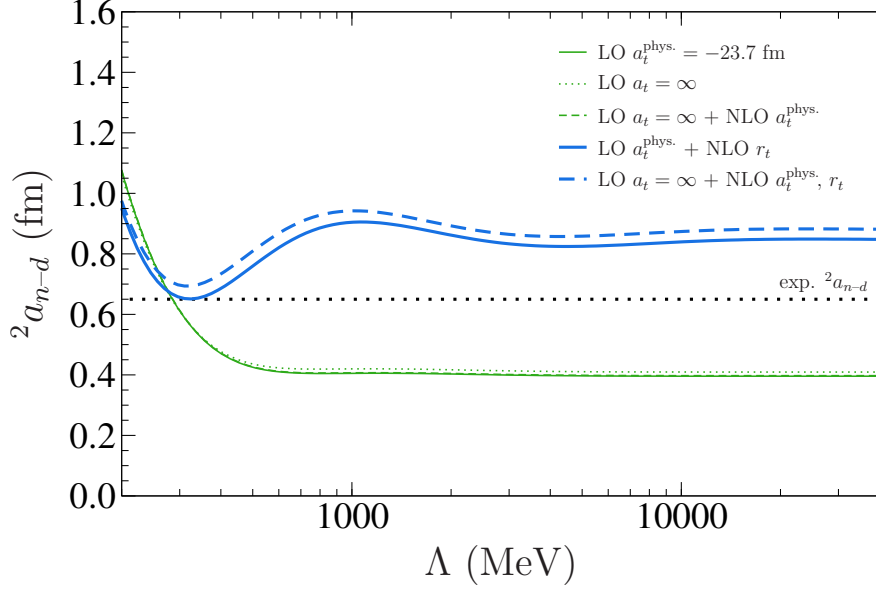


Figure 10:  $nd$  doublet-channel scattering length (in fm) as a function of the cutoff  $\Lambda$  (in MeV). Numerically, the limit in Eq. (60) has been taken by setting  $k = 0.01$  MeV. Notation as in Fig. 9.

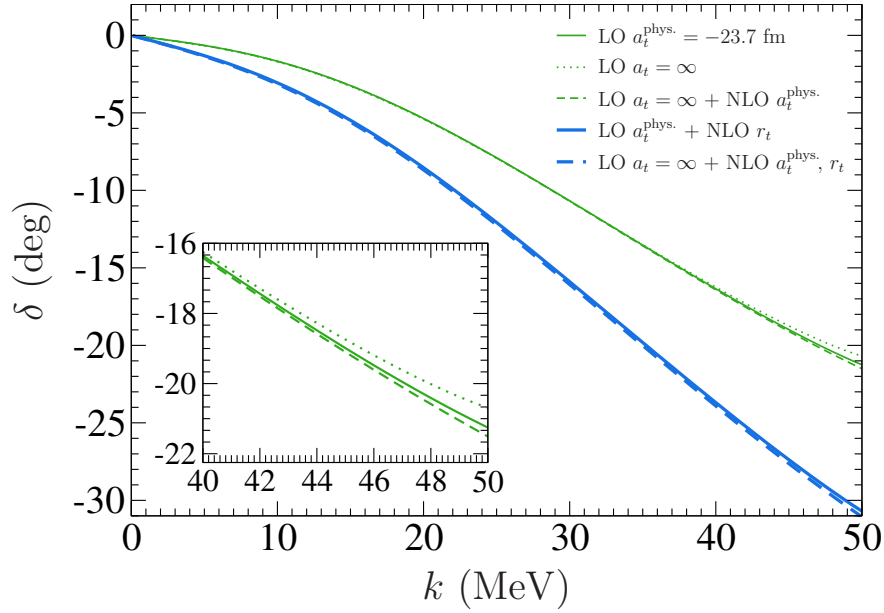


Figure 11:  $nd$  spin-doublet phase shift (in degrees) at LO and NLO as function of the center-of-mass momentum (in MeV). Notation as in Fig. 9.

proper renormalization of the three-body energy. This is in contrast with Ref. [26], which resums some Coulomb contributions already at LO and finds a logarithmic divergence at NLO when  $r_C = r_t$ .

The new contribution also provides a sizable (as compared to the total energy splitting) modification of the incomplete perturbative results of Ref. [54]. It brings the full perturbative result very close to the non-perturbative leading-order calculation of Ref. [54], which extended the results of Ref. [49] to much larger cutoff values. This establishes that Coulomb

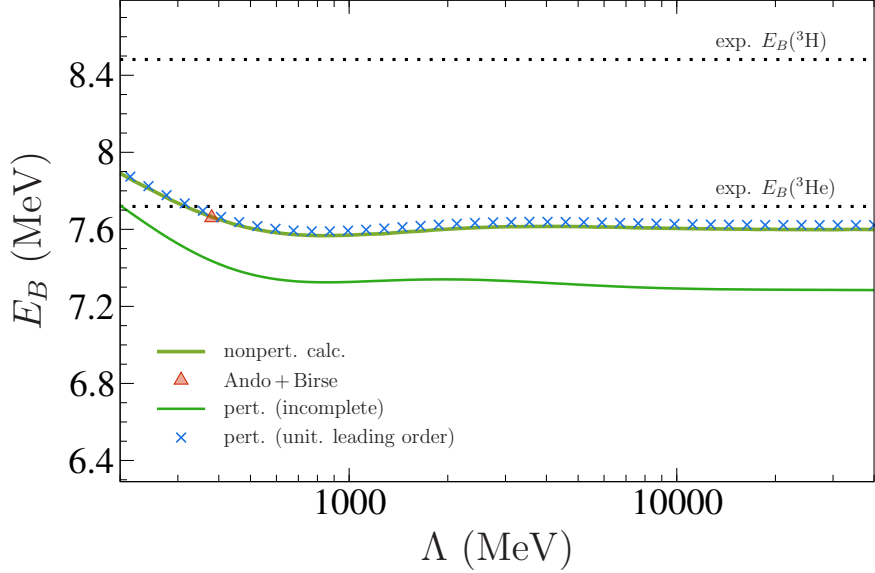


Figure 12: Results for the  ${}^3\text{He}$  binding energy (in MeV) as a function of the cutoff (in MeV). The upper solid curve shows the result of the nonperturbative calculation presented in Ref. [54]; the result of Ref. [49] is shown as a red triangle. The incomplete perturbative result of Ref. [54] is given by the lower solid line. Crosses represent the new complete perturbative calculation up to linear order in the spin-singlet scattering lengths. For comparison, dotted horizontal lines indicate the experimental values for the  ${}^3\text{H}$  and  ${}^3\text{He}$  binding energies. The photon mass  $\lambda$  has been linearly extrapolated to zero.

effects really are a completely perturbative correction in the  ${}^3\text{He}$  bound state compared to the  ${}^3\text{H}$ . We stress that “leading-order” means something different in that paper than in the new approach presented here: Ref. [54], as pionless calculations preceding it, resums certain Coulomb effects and includes the scattering length in the leading-order spin-singlet propagators, whereas we take those in the unitarity limit and only include the finite scattering lengths as perturbative corrections. At the same time, our calculation thus shows that this is a good approximation, as expected from the  $\aleph_0/Q$  expansion, which embodies the fact that these scattering lengths are very large.

At  $\text{N}^2\text{LO}$  and higher, isospin-breaking effects from the quark masses and higher-order electromagnetic effects will contribute. For example, the  $\mathcal{O}(\alpha^2)$  Coulomb contribution is attractive and tends to reduce the splitting found at NLO. Unfortunately, further shorter-range interactions will appear.  $NN$  input can, to some extent, be determined from  $NN$  data. Even in this case, however, there may be an isospin-breaking three-body force needed for proper renormalization. At that point, one can no longer predict the binding energy difference, unless one can determine this force’s parameter from another isospin-violating observable.

One of the higher-order effects comes from isospin violation in the effective ranges. At our NLO there is no isospin breaking in these, so  $r_t = r_C$  and there are no effective-range effects in the binding energy difference. This is a feature by construction in our new approach: our LO state is isospin-symmetric in the spin-singlet channels, so perturbative corrections from isospin-symmetric ranges exactly cancel via the NLO adjustment of the existing three-nucleon force that keeps the triton in the right place. Once one includes isospin breaking



Figure 13: Combined “Coulomb + range” corrections contributing to the trinucleon binding energy in perturbation theory, a higher-order effect in our expansion.

in the spin-singlet ranges,  $r_t \neq r_C$ , at some higher order, one recovers again the linear divergence (as a function of the ultraviolet cutoff  $\Lambda$ ) that has been identified in Ref. [26].

Further contributions that are proportional to the effective ranges come from the direct coupling of photons to the dibaryon fields, which are generated by the covariant derivatives in Eqs. (5) and (6). The corresponding diagrams are shown in Fig. 13. The expressions for these diverge logarithmically as a function of the momentum cutoff  $\Lambda$ , as identified in Refs. [26, 52, 54]. Essentially, the scaling of the diagrams in Fig. 13 is the same as for the proton bubble with a single photon exchange that we discuss in Sec. III C. Whereas in that case we had momentum-independent vertices and a single nucleon propagator  $\sim q^{-2}$  left in each loop (after carrying out the energy integrals), we now get a factor  $1/q$  each from the ultraviolet behavior of the dibaryon propagators and trinucleon vertices, respectively. Compared to the Coulomb correction (67) the diagrams shown in Fig. 13 are suppressed by  $Q/\Lambda_\pi$ . This relative ordering is in fact exactly the same as in previous calculations [25, 26, 54], but in our new counting scheme it means that these diagrams are N<sup>2</sup>LO.

Thus, these two divergences associated with the effective ranges appear at higher orders in our approach. Note that Ref. [26] contains a third source of divergence which is linear in the effective ranges: the interference between non-perturbative Coulomb and perturbative range effects. This additional logarithmic divergence occurs because Ref. [26] employs the full Coulomb-dressed dibaryon propagator at leading order. We emphasize that this divergence is absent in our new approach where all Coulomb contributions are treated perturbatively. We see here an example of the more general fact that, when singular interactions are involved, the cutoff dependence of perturbative diagrams is not necessarily the same as that of the resummed series. As a consequence, as noted above, no new three-body interaction is needed for renormalization at NLO in our new counting.

The discussion here can be generalized to other isospin-violating effects. Our expansion for explicit electromagnetic effects is in powers of  $\alpha M_N/Q$ , which we are counting as  $\aleph_0/Q$  and pairing, for simplicity, with the standard pionless EFT expansion  $Q/\Lambda_\pi$ . In addition to photon exchange, there are “indirect” electromagnetic effects that take place at short distances and appear in the Lagrangian as interactions among nucleons. Moreover, the up-down quark mass difference also generates isospin-breaking interactions. The form of the interactions are dependent on the way isospin is broken [65, 66]. Since the quark masses break charge symmetry (a rotation of  $\pi$  around the second axis in isospin space), their low-energy footprints will break charge symmetry as well, at least in first-order perturbation theory. In contrast, electromagnetic interactions break isospin more generally.

The most obvious consequence of isospin-breaking interactions is the neutron-proton mass splitting  $\delta M_N$ . We can estimate this as  $\delta M_N = \mathcal{O}(\alpha M_N/(4\pi), m_u - m_d)$ , where we included a  $4\pi$  expected from a photon loop. It is well known that these effects have opposite signs and

are comparable in magnitude, but, as indicated by this estimate, the quark-mass contribution is somewhat larger and makes the neutron heavier. One might worry that this splitting, appearing as a mass term in the Lagrangian, should be compared to the kinetic terms shown in Eq. (1). However, the nucleon mass splitting term can be removed by a redefinition of the nucleon field [67], and once this is done the splitting appears only in the kinetic term itself. It is thus  $\mathcal{O}(\delta M_N/M_N)$  relative to leading order, a very small effect.

The dominant isospin-breaking effects are expected to appear in the short-range two-nucleon interactions, represented in Eq. (1) via dibaryon fields. With the choice in Eq. (9), one counts the dibaryon residual masses as small scales, *e.g.*,  $\sigma_t = \mathcal{O}(\aleph_0)$ . To first order in the isospin-breaking parameters,  $\sigma_{t,nn} - \sigma_t$  is proportional to  $m_u - m_d$ , while  $\sigma_{t,pp} - \sigma_t$  is proportional to both  $(m_u - m_d)$  and  $\alpha M_N$ . The largest sizes they are expected to have are  $(\sigma_{t,nn} - \sigma_t)/\sigma_t = \mathcal{O}((m_u - m_d)/\aleph_0)$  and  $(\sigma_{t,pp} - \sigma_t)/\sigma_t = \mathcal{O}(\alpha M_N/\aleph_0, (m_u - m_d)/\aleph_0)$ . The electromagnetic contribution in the  $pp$  channel of  $\mathcal{O}(\alpha M_N/\aleph_0) = \mathcal{O}(1)$  is just the one required to renormalize Coulomb treated as NLO; the  $\alpha M_N$  appears explicitly in Eq. (45). This counting is consistent since it yields  $a_t/a_C - 1 = \mathcal{O}(1)$ , while empirical values give  $a_t/a_C - 1 \approx 2$ .

How we count the quark-mass effects is a matter of choice, since  $m_u - m_d$  is at the QCD level an independent parameter. The estimate above suggests  $a_t/a_{t,nn} - 1 = \mathcal{O}((m_u - m_d)/\aleph_0) \sim 0.3$ , again consistent with the standard value  $a_{t,nn} \simeq -18.7$  fm [68], which gives  $a_t/a_{t,nn} - 1 \approx 0.25$ . However, there are significant uncertainties in the value of  $a_{t,nn}$ . For example, a value  $a_{t,nn} \simeq -16.1$  fm has also been obtained [69], which would mean more significant quark mass effects. Conversely, a value closer to  $a_t$  would more clearly indicate  $m_u - m_d$  as a separate scale, much smaller than  $\aleph_0$ . In Ref. [48] a pionless EFT analysis of the trinucleon energy splitting  $\Delta E$  was carried out at LO in the standard power counting with an additional quark-mass, isospin-breaking  $NN$  interaction. In this case,  $\Delta E$  is correlated with  $a_{t,nn}$ , and one can use the experimental value of the former to determine the latter. It was found that  $a_{t,nn} \simeq -(22.9 \pm 4.1)$  fm, which gives  $a_t/a_{t,nn} - 1$  ranging from  $-0.1$  to  $0.25$ . This suggests that the pairing  $m_u - m_d \sim \alpha M_N/4\pi$  that one could infer from the nucleon mass splitting can be applied to  $NN$  interactions as well, which results in quark-mass effects about an order of magnitude below electromagnetic ones. We therefore took in this paper the standpoint that these are N<sup>2</sup>LO effects and do not contribute to the order we were working. Once the most important quark mass contribution is relegated to an order where new, undetermined counterterms appear, it is no longer possible to constrain  $a_{t,nn}$  from  $\Delta E$  [53].

For higher terms in the  $Q/\Lambda_\pi$  expansion, similar arguments can be used, but now taking into account that their parameters are determined by the high scales as given by the pionless EFT power counting. For example [4, 5, 7, 9],  $c_t = \mathcal{O}(M_N/\Lambda_\pi)$ , so we expect  $(c_{t,nn} - c_t)/c_t = \mathcal{O}((m_u - m_d)/\Lambda_\pi)$  and  $(c_{t,pp} - c_t)/c_t = \mathcal{O}(\alpha M_N/\Lambda_\pi, (m_u - m_d)/\Lambda_\pi)$ . These relations indicate a suppression of  $\mathcal{O}(\aleph_0/\Lambda_\pi)$  relative to breaking in  $\sigma_{t(..)}$ . They imply  $r_C/r_t - 1 = \mathcal{O}(\alpha M_N/\Lambda_\pi) \sim 0.05$ , in agreement with  $r_C/r_t - 1 \approx 0.02$  from empirical values. Thus, it is consistent to take the electromagnetic isospin-breaking range as an N<sup>2</sup>LO effect, with the prediction (48) valid up to about 5%. As we pointed out above, a linear divergence appears in the three-nucleon system which then requires a new, isospin-breaking three-body force at the same order.



Our result for the  ${}^3\text{He}$  binding energy is

$$E_B({}^3\text{He})^{\text{LO+NLO}} = E_B({}^3\text{H}) + \Delta E^{\text{NLO}} \\ = 8.48 \text{ MeV} - (0.86 \pm 0.17) \text{ MeV} = (7.62 \pm 0.17) \text{ MeV}, \quad (74)$$

where we estimated the error in the energy difference as  $\mathcal{O}(\alpha M_N/Q, (m_d - m_u)/\Lambda_0) \sim 20\%$ —slightly larger than the ratio NLO/LO. Eq. (74) represents 98.7% of the observed value,  $E_B({}^3\text{He})^{\text{exp}} \approx 7.72 \text{ MeV}$ . There is room for higher-order contributions, but most of the splitting is accounted for at NLO.

We emphasize that the error in Eq. (74) should be understood as a rough estimate of higher-order contributions. The above value comes from taking the mean of  $a_C$  and  $a_t$  for  $1/\Lambda_0$ . By using the physical value for  $a_C$  as NLO input, we are overestimating the magnitude of electromagnetic effects, because  $\text{N}^2\text{LO}$  corrections of both electromagnetic and quark-mass origin contribute to the  $pp$  scattering length. Potential-model calculations of photon exchange (for example, Ref. [70]) tend to give a  $\Delta E$  consistent with an almost model-independent estimate of about 680 keV [71], but not the full isospin violation in the  $NN$  scattering lengths. Our result cannot be directly compared with these older perturbative-photon calculations because we include also shorter-range interactions—as required to ensure renormalization—that give the measured  $pp$  scattering length. However, the EFT allows us to directly study effects when  $a_C$  is closer to  $a_t$ , effectively simulating a potential-model calculation with an interaction that does not give the physical splitting in the scattering lengths. For example we find that  $a_C = -9.0$  ( $-10.0$ ) fm leads to a trinucleon splitting of about 700 (600) keV, and we can thus confirm that the older calculations are consistent with an uncertainty of about 20% in  $a_C$ , in line with our estimate of higher-order contributions above.

## VI. SUMMARY AND OUTLOOK

In this work, we have established a rearrangement of the perturbative expansion in pionless effective field theory that takes the spin-singlet nucleon–nucleon channels in the unitarity limit. Not only does this allow us to demonstrate quantitatively that nature is very close to this scenario, it also enables us to include Coulomb corrections perturbatively on the same footing. An important ingredient to this is the consistent isolation of the divergent one-photon piece in the  $pp$  sector, which then guarantees the renormalization of the corresponding contribution in the three-nucleon sector.

By studying the trinucleon bound-state sector, we confirm that the new perturbative expansion works very well: both the Phillips line and doublet-channel  $nd$  phase shifts are barely changed by perturbative corrections that include the actual finiteness of these quantities, proving that the new leading order is a good starting point for a perturbative expansion. By comparison with previous nonperturbative calculations of the energy splitting in the  ${}^3\text{H}$ – ${}^3\text{He}$  iso-doublet, we furthermore show that the Coulomb interaction is indeed a completely perturbative effect in these bound states. Our new NLO with effective-range corrections set to zero is almost on top of previous leading-order calculations that resum certain (but not all) Coulomb contributions. The same holds when isospin-symmetric ranges are included. There is no new divergence at this order, which allows us to predict the energy splitting as  $\Delta E^{\text{NLO}} = -(0.86 \pm 0.17) \text{ MeV}$ , to be compared with the experimental value  $\Delta E^{\text{exp}} \simeq -0.764 \text{ MeV}$ .

The main point of our reorganization is that, by treating small quantities in perturbation theory, we remove inessential parameters from the lowest orders. For example, a 30% accuracy for nuclear observables susceptible to pionless EFT should be obtained from only two parameters at LO, with four other parameters at NLO ensuring a 10% accuracy or better. An investigation of this reorganization in heavier systems is our next goal.

Further improvement comes from higher orders. Isospin-symmetric effective ranges do not contribute to the  ${}^3\text{H}$ – ${}^3\text{He}$  energy difference. The inclusion of isospin breaking in these effective ranges will recover the previously identified divergence generated by this effect; the same is true for contributions that are of the same order in  $\alpha$  as other Coulomb effects included here, but suppressed further by  $\rho_d, r_t \sim 1/\Lambda_\pi$ . Confirming that these contributions are indeed best accounted for at N<sup>2</sup>LO, and carrying out a fully consistent renormalization at this order, is beyond the scope of this work and relegated to future investigations.

## Acknowledgments

We thank Giovanni Chirilli, Sid Coon, Dick Furnstahl, Doron Gazit, and Johannes Kirscher for useful discussions, and the latter also for comments on the manuscript. Three of us (SK, HWG, UvK) are grateful to the organizers and participants of the workshop LATTICE NUCLEI, NUCLEAR PHYSICS AND QCD – BRIDGING THE GAP at the ECT\*, Trento (Italy), for stimulating presentations and an atmosphere which inspired the completion of this article. This material is based upon work supported in part by the NSF under Grant No. PHY-1306250 (SK), by the NUCLEI SciDAC Collaboration under DOE Grant DE-SC0008533 (SK), by the Dean’s Research Chair programme of the Columbian College of Arts and Sciences of The George Washington University (HWG), by the U.S. Department of Energy, Office of Science, Office of Nuclear Physics, under Award Numbers DE-FG02-95ER-40907 and DE-SC0015393 (HWG) and DE-FG02-04ER41338 (UvK), by the BMBF under contracts 05P12PDFTE and 05P15RDFN1 (HWH), and by the Helmholtz Association under contract HA216/EMMI (HWH).

## Appendix A: The Coulomb bubble integrals

### 1. Single-photon bubble

Let us consider the bubble integral with a single Coulomb-photon insertion. The original integral is given by

$$\delta I_0(k) = 4\pi M_N^2 \int \frac{d^3 q_1}{(2\pi)^3} \int \frac{d^3 q_2}{(2\pi)^3} \frac{1}{k^2 - q_1^2 + i\epsilon} \frac{1}{q_2^2 + \lambda^2} \frac{1}{k^2 - (\mathbf{q}_1 + \mathbf{q}_2)^2 + i\epsilon}. \quad (\text{A1})$$

This has been calculated by Kong and Ravndal [39] using dimensional regularization. However, their result is not entirely correct, so we repeat the calculation in Sec. A 1 a. In Sec. A 1 b, we carry out the calculation with a simple momentum cutoff, as used in the main part of the paper.

*a. Dimensional regularization*

Following Kong and Ravndal, we set  $k^2 = -\gamma^2$ . Going to  $d = 3 - \epsilon$  dimensions, and introducing the renormalization scale  $\mu$  and a Feynman parameter, we get

$$\begin{aligned}\delta I_0 &= 4\pi\alpha M_N^2 \left(\frac{\mu}{2}\right)^{2\epsilon} \int \frac{d^d q_2}{(2\pi)^d} \frac{1}{q_2^2 + \lambda^2} \int_0^1 dx \int \frac{d^d q_1}{(2\pi)^d} \frac{1}{[x(\gamma^2 + q_1^2) + (1-x)(\gamma^2 + (\mathbf{q}_1 + \mathbf{q}_2)^2)]^2} \\ &= 4\pi\alpha M_N^2 \left(\frac{\mu}{2}\right)^{2\epsilon} \frac{\Gamma(\frac{1}{2} + \frac{\epsilon}{2})}{(4\pi)^{\frac{3-\epsilon}{2}} \Gamma(2)} \int_0^1 dx \int \frac{d^d q}{(2\pi)^d} \frac{1}{(q^2 + \lambda^2) [(x - x^2)q^2 + \gamma^2]^{\frac{1}{2} + \frac{\epsilon}{2}}}.\end{aligned}\quad (\text{A2})$$

Further following Kong and Ravndal we set  $a \equiv \gamma^2/(x - x^2)$  and introduce a second Feynman parameter to write

$$\begin{aligned}\delta I_0 &= 4\pi\alpha M_N^2 \left(\frac{\mu}{2}\right)^{2\epsilon} \frac{\Gamma(\frac{1}{2} + \frac{\epsilon}{2})}{(4\pi)^{\frac{3-\epsilon}{2}} \Gamma(2)} \int_0^1 dx \frac{1}{(x - x^2)^{\frac{1}{2} + \frac{\epsilon}{2}}} \\ &\quad \times \int_0^1 d\omega \int \frac{d^d q}{(2\pi)^d} \frac{\omega^{-\frac{1}{2} + \frac{\epsilon}{2}}}{[(1 - \omega)(q^2 + \lambda^2) + \omega(q^2 + a)]^{\frac{3}{2} + \frac{\epsilon}{2}}}.\end{aligned}\quad (\text{A3})$$

Noting that

$$(1 - \omega)(q^2 + \lambda^2) + \omega(q^2 + a) = q^2 + (1 - \omega)\lambda^2 + \omega \frac{\gamma^2}{x - x^2}, \quad (\text{A4})$$

we can carry out the integral and arrive at

$$\delta I_0 = 4\pi\alpha M_N^2 \left(\frac{\mu}{2}\right)^{2\epsilon} \frac{\Gamma(\frac{1}{2} + \frac{\epsilon}{2})\Gamma(\epsilon)}{(4\pi)^{3-\epsilon} \Gamma(2)\Gamma(\frac{3}{2} + \frac{\epsilon}{2})} \int_0^1 dx \frac{1}{(x - x^2)^{\frac{1}{2} + \frac{\epsilon}{2}}} \int_0^1 d\omega \frac{\omega^{-\frac{1}{2} + \frac{\epsilon}{2}}}{\left((1 - \omega)\lambda^2 + \omega \frac{\gamma^2}{x - x^2}\right)^\epsilon}.\quad (\text{A5})$$

Let us consider first the case  $\lambda = 0$ , as done by Kong and Ravndal. In that case, the two integrals are

$$\begin{aligned}\int_0^1 dx \frac{1}{(x - x^2)^{\frac{1}{2} + \frac{\epsilon}{2}}} \int_0^1 d\omega \frac{\omega^{-\frac{1}{2} + \frac{\epsilon}{2}}}{\left(\omega \frac{\gamma^2}{x - x^2}\right)^\epsilon} &= \gamma^{-2\epsilon} \int_0^1 dx (x - x^2)^{-\frac{1}{2} + \frac{\epsilon}{2}} \int_0^1 d\omega \omega^{-\frac{1}{2} - \frac{\epsilon}{2}} \\ &= \gamma^{-2\epsilon} \frac{2^{-\epsilon} \sqrt{\pi} \Gamma(\frac{1}{2} + \frac{\epsilon}{2})}{\Gamma(1 + \frac{\epsilon}{2})} \frac{2}{1 - \epsilon}.\end{aligned}\quad (\text{A6})$$

Hence,

$$\begin{aligned}\delta I_0^{\lambda=0} &= \frac{\alpha M_N^2}{8\pi^{3/2}} \left(\frac{\pi\mu^2}{2\gamma^2}\right)^\epsilon \frac{[\Gamma(\frac{1}{2} + \frac{\epsilon}{2})]^2 \Gamma(\epsilon)}{\Gamma(2) \Gamma(\frac{3}{2} + \frac{\epsilon}{2}) \Gamma(1 + \frac{\epsilon}{2})} \frac{1}{1 - \epsilon} \\ &= \frac{\alpha M_N^2}{4\pi} \left[ \frac{1}{\epsilon} + 2 \log \frac{\mu\sqrt{\pi}}{2\gamma} - C_E \right] + \mathcal{O}(\epsilon).\end{aligned}\quad (\text{A7})$$

Note that this differs slightly from the result obtained by Kong and Ravndal due to an error<sup>5</sup> in Ref. [39]. If we keep the photon-mass term, the integrals over the Feynman parameters cannot be separated. After a couple of steps one arrives at

$$\begin{aligned} \int_0^1 dx \frac{1}{(x-x^2)^{\frac{1}{2}+\frac{\epsilon}{2}}} \int_0^1 d\omega \frac{\omega^{-\frac{1}{2}+\frac{\epsilon}{2}}}{\left((1-\omega)\lambda^2 + \omega \frac{\gamma^2}{x-x^2}\right)^\epsilon} \\ = 2\pi + 2\pi \epsilon \left[ 1 + 2 \log \frac{\mu}{2\gamma} + 2 \log \left( 1 + \frac{\lambda}{2\gamma} \right) \right] + \mathcal{O}(\epsilon^2), \end{aligned} \quad (\text{A8})$$

so eventually we get

$$\delta I_0 = \frac{\alpha M_N^2}{4\pi} \left[ \frac{1}{\epsilon} + 2 \log \frac{\mu\sqrt{\pi}}{2\gamma} - 2 \log \left( 1 + \frac{\lambda}{2\gamma} \right) - C_E \right] + \mathcal{O}(\epsilon), \quad (\text{A9})$$

which reduces to Eq. (A7) when  $\lambda = 0$ .

#### *b. Simple momentum cutoff*

We now consider the integral with a simple momentum cutoff  $\Lambda$ . In that case, Eq. (A1) (with  $\lambda = 0$ ) becomes

$$\delta I_0^{\lambda=0}(k) = 4\pi\alpha M_N^2 \int^\Lambda \frac{d^3 q_1}{(2\pi)^3} \int^\Lambda \frac{d^3 q_2}{(2\pi)^3} \frac{1}{k^2 - q_1^2 + i\epsilon} \frac{1}{q_2^2} \frac{1}{k^2 - (\mathbf{q}_1 + \mathbf{q}_2)^2 + i\epsilon}, \quad (\text{A10})$$

or, more conveniently for the present calculation,<sup>6</sup>

$$\delta I_0^{\lambda=0}(k) = 4\pi\alpha M_N^2 \int^\Lambda \frac{d^3 q_1}{(2\pi)^3} \int^\Lambda \frac{d^3 q_2}{(2\pi)^3} \frac{1}{k^2 - q_1^2 + i\epsilon} \frac{1}{(\mathbf{q}_1 - \mathbf{q}_2)^2} \frac{1}{k^2 - q_2^2 + i\epsilon}. \quad (\text{A11})$$

This is logarithmically divergent, so based on dimensional analysis we know that

$$\delta I_0^{\lambda=0}(k) = \frac{\alpha M_N^2}{4\pi} \left[ A \log \frac{\Lambda}{k} + B + \mathcal{O}(k/\Lambda) \right], \quad (\text{A12})$$

with some dimensionless constants  $A$  and  $B$ . To determine these, we first carry out the angular integrals in Eq. (A11) (all except one of which are trivial). As done in the calculation with dimensional regularization, we also analytically continue to  $k = i\gamma$ ,  $\gamma > 0$  and let  $\epsilon \rightarrow 0$ . This gives

$$\delta I_0^{\lambda=0}(k) = \frac{\alpha M_N^2}{\pi^2} \int_0^\Lambda dq_1 q_1^2 \int_0^\Lambda dq_2 q_2^2 \frac{\log [(q_1^2 + q_2^2 + 2q_1 q_2)/(q_1^2 + q_2^2 - 2q_1 q_2)]}{2q_1 q_2 (q_1^2 + \gamma^2)(q_2^2 + \gamma^2)}. \quad (\text{A13})$$

<sup>5</sup> The argument of the Gamma function in the denominator of Eq. (100) in Ref. [39] should be  $3 - d/2$  instead of  $2 - d/2$ .

<sup>6</sup> The shift involved in this rearrangement, which is equivalent to a different momentum assignment in the corresponding Feynman diagram, should only affect the terms suppressed by inverse powers of the cutoff.

Carrying out the integration over  $q_1$  gives

$$\delta I_0^{\lambda=0}(k) = -\frac{\alpha M_N^2}{2\pi^2} \int_0^\Lambda \frac{dq q}{q^2 + \gamma^2} \times \left[ \log\left(\frac{\Lambda - q}{\Lambda + q}\right) \log\left(\frac{\Lambda^2 + \gamma^2}{q^2 + \gamma^2}\right) \right. \\ \left. + \text{Li}_2\left(\frac{q - \Lambda}{q - i\gamma}\right) - \text{Li}_2\left(\frac{q + \Lambda}{q - i\gamma}\right) + \text{Li}_2\left(\frac{q - \Lambda}{q + i\gamma}\right) - \text{Li}_2\left(\frac{q + \Lambda}{q + i\gamma}\right) \right], \quad (\text{A14})$$

where we have renamed the second loop momentum  $q_2 \rightarrow q$ . The remaining integral can be carried out using an indefinite integral which is given by a complicated sum of logarithms and polylogarithms. We do not write this out here, but simply note that the final result can be asymptotically expanded for large  $\Lambda$  to yield

$$A = 1 \quad \text{and} \quad B = -\left(\log 2 + \frac{7\zeta(3)}{2\pi^2}\right), \quad (\text{A15})$$

so that overall

$$\delta I_0^{\lambda=0} = \frac{\alpha M_N^2}{4\pi} \left[ \log \frac{\Lambda}{\gamma} - C_\zeta + \mathcal{O}(k/\Lambda) \right], \quad (\text{A16})$$

where for convenience we have defined

$$C_\zeta = \log 2 + \frac{7\zeta(3)}{2\pi^2} \approx 1.11943. \quad (\text{A17})$$

Adding  $0 = \log(\alpha M_N/2) - \log(\alpha M_N/2)$  to Eq. (A16) we arrive at Eq. (41).

## 2. Fully dressed bubble

The fully dressed  $pp$  bubble shown in Fig. 3 resums the contribution of an arbitrary number of Coulomb-photon exchanges. We discuss it here in a number of schemes, starting with the results of Kong and Ravndal [39], who used both dimensional regularization and a simple momentum cutoff. As discussed in the main text, Ref. [39] splits up the full bubble integral into a finite piece that gives the function  $H(\eta)$  in the Coulomb-modified effective range expansion, and a divergent piece, which is the only integral that is regularized. In dimensional regularization, Kong and Ravndal find, for  $d = 3 - \epsilon$ ,

$$J_0^{\text{div}} = -M_N \left(\frac{\mu}{2}\right)^\epsilon \frac{2\pi^{d/2}}{(2\pi)^d \Gamma(d/2)} \int_0^\infty dq q^{d-3} \frac{2\pi\eta(q)}{e^{2\pi\eta(q)} - 1} \frac{1}{q^2} \\ = \frac{\alpha M_N^2}{4\pi} \left( \frac{1}{\epsilon} + \log \frac{\mu\sqrt{\pi}}{\alpha M_N} + 1 - \frac{3}{2}C_E \right) - \frac{\mu M_N}{4\pi}, \quad (\text{A18})$$

where the result in the second line is obtained through the substitution  $x = 2\pi\eta(q)$ , which leads to the integral

$$\int_0^1 dx \frac{x^{\epsilon-1}}{e^x - 1} = \Gamma(\epsilon)\zeta(\epsilon). \quad (\text{A19})$$

A subsequent expansion of the Zeta and Gamma functions gives the PDS pole in  $d = 2$  and the  $1/\epsilon$  divergence for  $d \rightarrow 3$ , respectively. With a simple cutoff, the result is given in Eq. (34).

Note that Kong and Ravndal only consider the full series (empty bubble, one photon exchange, two photon exchanges, *etc.*) shown in Fig. 3 at once, although the logarithmic divergence really comes only from the single-photon contribution.<sup>7</sup> This leads to the puzzling result that while the  $1/\epsilon$  divergences for the single-photon and fully dressed bubbles (see Eqs. (A7) and (A18), respectively) agree (same prefactor/residue), the logarithmic pieces that depend on the renormalization scale  $\mu$ , as well as the constant terms, do not. Such an effect can be created by splitting up a formally divergent expression and applying the regularization only to a part of it. To see this issue, note for example that the integrand in Eq. (A18) cannot be expanded to order  $\alpha$  to recover the single-photon result.

While in Ref. [39] this does not actually play a role—although they discuss the single-photon bubble for illustration, the authors eventually only use the fully dressed bubble for the matching to the Coulomb-modified scattering length—in the current work we require a scheme that is consistent throughout, *i.e.*, we want to isolate the divergent single-photon piece within the fully dressed bubble. In Sec. A 3 we first establish in configuration space that the logarithmically-divergent pieces should indeed be the same for both bubble diagrams, before we finally discuss in Sec. A 4 our approach of using the Coulomb T-matrix to isolate the the single-photon contribution, while still giving a closed expression for the rest.

### 3. Configuration space

Let us consider the two bubble integrals in configuration space in order to analyze their divergences more carefully. To this end, note that what we really want to calculate is the zero-to-zero Green's functions [39, 40],

$$J_0(k) = G_C(E; \mathbf{r}' = \mathbf{0}, \mathbf{r} = \mathbf{0}) \quad , \quad E = k^2/M_N \quad . \quad (\text{A20})$$

Of course, this is infinite, so we want to isolate the divergence by starting from a finite separation and considering the case where it goes to zero. This procedure only deals with well-defined finite quantities, so we expect it to avoid subtleties associated with splitting up formally infinite terms.

The Coulomb Green's function satisfies the equation

$$\frac{1}{2\mu} \left( \Delta_r + \frac{2\mu\alpha}{r} + k^2 \right) G_C(E; \mathbf{r}, \mathbf{r}') = \delta^{(3)}(\mathbf{r} - \mathbf{r}') \quad , \quad (\text{A21})$$

in exact correspondence to the free case,

$$\frac{1}{2\mu} (\Delta_r + k^2) G_0^{(+)}(E; \mathbf{r}, \mathbf{r}') = \delta^{(3)}(\mathbf{r} - \mathbf{r}') \quad . \quad (\text{A22})$$

For the present case, the reduced mass is  $\mu = M_N/2$ . This Green's function is known analytically [72, 73] when one argument is set to zero. Adjusting to agree with the conventions used in Ref. [52], we have

$$G_C(E; \mathbf{r}' = \mathbf{0}, \mathbf{r}) = -2\mu \frac{\Gamma(1 - i\eta) W_{i\eta; 1/2}(-2ikr)}{4\pi r} \quad , \quad \eta = \frac{\alpha\mu}{k} \quad . \quad (\text{A23})$$

---

<sup>7</sup> In addition, the PDS pole in  $d = 2$  corresponds to the linear divergence of the empty bubble.

Expanding first the Whittaker function around  $r = 0$ , and subsequently the whole right-hand side in powers of  $\alpha$ , we find

$$G_C(E; \mathbf{r}' = \mathbf{0}, \mathbf{r}) = -\frac{M_N}{4\pi} \left[ \frac{1}{r} + ik + \alpha M_N (1 - C_E - \log(-2ikr)) \right] + \mathcal{O}(r). \quad (\text{A24})$$

The  $1/r$  and  $\log(r)$  terms in the above expression directly correspond to the linear and logarithmic divergences that we found previously in momentum space.

The free Green's function, *i.e.*, the solution to Eq. (A22), is given by

$$G_0^{(+)}(E; \mathbf{r}, \mathbf{r}') = \langle \mathbf{r} | \hat{G}_0^{(+)}(E) | \mathbf{r}' \rangle = -\frac{\mu}{2\pi} \frac{e^{ik|\mathbf{r}-\mathbf{r}'|}}{|\mathbf{r}-\mathbf{r}'|}. \quad (\text{A25})$$

The first two terms in Eq. (A24) come from, with  $\mu = M_N/2$ ,

$$G_0^{(+)}(E; \mathbf{r}' = \mathbf{0}, \mathbf{r}) = -\frac{M_N}{4\pi} \left[ \frac{1}{r} + ik \right] + \mathcal{O}(r). \quad (\text{A26})$$

This corresponds to the contribution of the empty bubble.

We now turn to the single-photon diagram and expect to find exactly the remaining divergence, because diagrams with two and more photons should be finite. What we have to calculate is thus

$$G_C^{(1)}(E; \mathbf{r}', \mathbf{r}) = \langle \mathbf{r} | \hat{G}_0^{(+)}(E) \hat{V}_C \hat{G}_0^{(+)}(E) | \mathbf{r}' \rangle, \quad (\text{A27})$$

where

$$\langle \mathbf{r} | \hat{V}_C | \mathbf{r}' \rangle = \delta^{(3)}(\mathbf{r} - \mathbf{r}') \frac{\alpha}{r} \quad (\text{A28})$$

is the Coulomb potential. Setting  $k = \sqrt{2\mu E + i\epsilon}$  and  $\mathbf{r}' = \mathbf{0}$  in Eq. (A27) gives

$$G_C^{(1)}(E; \mathbf{0}, \mathbf{r}) = \frac{\alpha\mu^2}{2\pi} \int_0^\infty dr'' e^{ikr''} \int_{-1}^1 d\cos\theta \frac{e^{ik|\mathbf{r}-\mathbf{r}''|}}{|\mathbf{r}-\mathbf{r}''|}, \quad \mathbf{r}'' \cdot \mathbf{r} = r'' r \cos\theta, \quad (\text{A29})$$

where we have inserted identities to separate the operators and carried out the trivial integrals. The angular integral simply recovers the well-known expression for the  $S$ -wave projected free Green's function:

$$\int_{-1}^1 d\cos\theta \frac{e^{ik|\mathbf{r}-\mathbf{r}''|}}{|\mathbf{r}-\mathbf{r}''|} = -\frac{2}{k} \frac{e^{ikr_{>}} \sin(kr_{<})}{r'' r}, \quad r_{>} = \max(r, r''), \quad r_{<} = \min(r, r''). \quad (\text{A30})$$

The remaining integral in Eq. (A29) can then be done by splitting up the domain according to

$$\int_0^\infty dr'' = \int_0^r dr'' + \int_r^\infty dr''. \quad (\text{A31})$$

In each region,  $r_{<}$  and  $r_{>}$  are then uniquely defined. The first integral is

$$\int_0^r \frac{e^{ikr''} \sin(kr'')}{r''} dr'' = \frac{i}{2} \left( C_E + \log(2kr) - \text{Ci}(2kr) - i \text{Si}(2kr) \right), \quad (\text{A32})$$

in terms of the sine and cosine integrals [74], respectively

$$\text{Si}(z) = \int_0^z \frac{\sin(t)}{t} dt = \mathcal{O}(z), \quad (\text{A33a})$$

$$\text{Ci}(z) = -\int_z^\infty \frac{\cos(t)}{t} dt = C_E + \log z + \mathcal{O}(z^2). \quad (\text{A33b})$$

For the second integral we find

$$\int_r^\infty \frac{e^{2ikr''}}{r''} dr'' = \Gamma(-2ikr). \quad (\text{A34})$$

Combining the results, we get

$$G_C^{(1)}(E; \mathbf{r}' = \mathbf{0}, \mathbf{r}) = -\frac{\alpha\mu^2}{\pi kr} \left\{ \frac{ie^{ikr}}{2} \left[ C_E + \log(2kr) - \text{Ci}(2kr) - i \text{Si}(2kr) \right] + \sin(kr) \Gamma(-2ikr) \right\}. \quad (\text{A35})$$

Finally, expanding this around  $r = 0$  and inserting  $\mu = M_N/2$ , we arrive at

$$G_C^{(1)}(E; \mathbf{r}' = \mathbf{0}, \mathbf{r}) = -\frac{\alpha M_N^2}{4\pi} \left[ 1 - C_E - \log(-2ikr) \right] + \mathcal{O}(r). \quad (\text{A36})$$

This is exactly the term linear in  $\alpha$  in Eq. (A24).

#### 4. Fully dressed bubble with T-matrix expansion

Having established that the remaining divergence indeed comes exactly from the single-photon diagram, let us take another shot at consistently isolating it in a momentum-space calculation. To this end, note that the Coulomb Green's function satisfies the operator equation

$$\hat{G}_C(E) = \hat{G}_0^{(+)}(E) + \hat{G}_0^{(+)}(E) \hat{V}_C \hat{G}_C(E). \quad (\text{A37})$$

On the other hand, we have the Coulomb T-matrix defined by the Lippmann–Schwinger equation

$$\hat{T}_C(E) = \hat{V}_C + \hat{V}_C \hat{G}_0^{(+)}(E) \hat{T}_C(E). \quad (\text{A38})$$

With

$$\hat{V}_C \hat{G}_C(E) = \hat{T}_C(E) \hat{G}_0^{(+)}(E), \quad (\text{A39})$$

we can write Eq. (A37) as

$$\hat{G}_C(E) = \hat{G}_0^{(+)}(E) + \hat{G}_0^{(+)}(E) \hat{T}_C \hat{G}_0^{(+)}(E). \quad (\text{A40})$$

The advantage of this operation becomes apparent once we note that the Coulomb T-matrix is known in closed form. For example, in terms of the Coulomb potential in momentum space

$$V_C(\mathbf{p}, \mathbf{q}) = \frac{4\pi\alpha}{(\mathbf{p} - \mathbf{q})^2}, \quad (\text{A41})$$



one has

$$T_C(k; \mathbf{p}, \mathbf{q}) = \langle \mathbf{p} | \hat{T}_C | \mathbf{q} \rangle = V_C(\mathbf{p}, \mathbf{q}) \left\{ 1 - 2i\eta \int_1^\infty \left( \frac{s+1}{s-1} \right)^{-i\eta} \frac{ds}{s^2 - 1 - \epsilon} \right\}, \quad (\text{A42})$$

or

$$T_C(k; \mathbf{p}, \mathbf{q}) = V_C(\mathbf{p}, \mathbf{q}) \left\{ 1 - \Delta^{-1} \left[ {}_2F_1 \left( 1, i\eta, 1 + i\eta; \frac{\Delta - 1}{\Delta + 1} \right) - {}_2F_1 \left( 1, i\eta, 1 + i\eta; \frac{\Delta + 1}{\Delta - 1} \right) \right] \right\}, \quad (\text{A43})$$

with

$$\epsilon = \frac{(p^2 - k^2)(q^2 - k^2)}{k^2(\mathbf{p} - \mathbf{q})^2}, \quad \Delta^2 = 1 + \epsilon. \quad (\text{A44})$$

For these and a number of alternative representations, see for example Ref. [75]. Note that both Eq. (A42) and (A43) express the T-matrix as the Coulomb potential plus a remainder that summarizes the exchange of two and more photons,

$$T_C(k; \mathbf{p}, \mathbf{q}) = V_C(\mathbf{p}, \mathbf{q}) + T_C^\Delta(k; \mathbf{q}, \mathbf{p}). \quad (\text{A45})$$

Hence, we can write the fully resummed bubble integral as

$$J_0(k) = I_0(k) + \delta I_0(k) + \delta J_0(k), \quad (\text{A46})$$

where

$$I_0(k) = M_N \int \frac{d^3 q}{(2\pi)^3} \frac{1}{k^2 - q^2 + i\epsilon} \quad (\text{A47})$$

is the empty bubble,  $\delta I_0(k)$  is exactly the single-photon bubble calculated in Sec. A 1, and  $\delta J_0(k)$  remains to be investigated. The crucial point is that it is supposed to be ultraviolet finite.

The integral we have to evaluate is

$$\delta J_0(k) = M_N^2 \int \frac{d^3 p}{(2\pi)^3} \int \frac{d^3 q}{(2\pi)^3} \frac{T_C^\Delta(k; \mathbf{q}, \mathbf{p})}{(p^2 - k^2 - i\epsilon)(q^2 - k^2 - i\epsilon)}. \quad (\text{A48})$$

Noting that  $T_C^\Delta(k; \mathbf{q}, \mathbf{p})$  depends only on the angle between  $\mathbf{q}$  and  $\mathbf{p}$ , we can carry out all but one angular integral. The remaining one over  $\cos \theta$  is then an  $S$ -wave projection. Fortunately, partial-wave projections of the full Coulomb T-matrix are known in closed form [76, 77]. The  $S$ -wave result can be written as [77]

$$T_{C,0}(E = k^2/(2\mu); p, q) = \frac{i\pi}{\mu} \frac{k}{pq} \left[ {}_2F_1(1, i\eta, 1 + i\eta; a'a) - {}_2F_1(1, i\eta, 1 + i\eta; a/a') + {}_2F_1(1, i\eta, 1 + i\eta; 1/(a'a)) - {}_2F_1(1, i\eta, 1 + i\eta; a'/a) \right], \quad (\text{A49})$$

where

$$a = \frac{p - k}{p + k}, \quad a' = \frac{q - k}{q + k}. \quad (\text{A50})$$

With the projection of the Coulomb potential alone,

$$V_{C,0}(p, q) = \frac{2\pi\alpha}{pq} Q_0 \left( \frac{p^2 + q^2}{2pq} \right) = \frac{\pi\alpha}{pq} \log \left( \frac{2pq + p^2 + q^2}{2pq - p^2 - q^2} \right), \quad (\text{A51})$$

we can write

$$\delta J_0(k) = \left( \frac{M_N}{2\pi^2} \right)^2 \int dp p^2 \int dq q^2 \frac{T_{C,0}(E = k^2/(2\mu); p, q) - V_{C,0}(p, q)}{(p^2 - k^2 - i\varepsilon)(q^2 - k^2 - i\varepsilon)}. \quad (\text{A52})$$

This integral looks difficult to solve, but at the very least it can be evaluated numerically. We do this with a (large) momentum cutoff and a small imaginary part of  $k$  in place for regularization. Considering the real part, one finds that it is consistent with

$$\text{Re } \delta J_0(k) = -\frac{\alpha M_N^2}{4\pi} \left( \text{Re} \left\{ \psi(i\eta) + \frac{1}{2i\eta} \right\} + C_\Delta \right) \quad (\text{A53})$$

with a constant

$$C_\Delta \approx 0.579. \quad (\text{A54})$$

The level of agreement is demonstrated in Fig. 14(a). Note that Eq. (A53) contains the function  $H(\eta)$  except for the  $\log i\eta$  part. This agrees with what one would expect here because in the sum (A46) we already have a  $\log k$  term from the single-photon contribution  $\delta I_0(k)$ . Considering the imaginary part, we find that it agrees very well with

$$\text{Im } \delta J_0(k) = -\frac{\alpha M_N^2}{4\pi} \text{Im} \left\{ \psi(i\eta) + \frac{1}{2i\eta} \right\} + \frac{M_N k}{4\pi}, \quad (\text{A55})$$

as shown in Fig. 14(b). Altogether, we have thus established numerically that

$$\delta J_0(k) = -\frac{\alpha M_N^2}{4\pi} \left( \psi(i\eta) + \frac{1}{2i\eta} + C_\Delta \right) + \frac{M_N}{4\pi} i k. \quad (\text{A56})$$

We expect that increased numerical accuracy would yield  $C_\Delta \rightarrow C_E \approx 0.577216$ . The value in Eq. (A54) represents our most accurate result (obtained with a momentum cutoff of 16000 MeV and  $\text{Im} k = 0.05$  MeV); decreasing the former and increasing the latter gives larger values for  $C_\Delta$ , so indeed we see a convergence pattern.

- 
- [1] H. A. Bethe, Phys. Rev. **76** (1949) 38.
  - [2] H. A. Bethe and R. Peierls, Proc. Roy. Soc. **A148** (1935) 146; *ibid.* **A149** (1935) 176.
  - [3] P. F. Bedaque and U. van Kolck, Phys. Lett. B **428** (1998) 221 [nucl-th/9710073].
  - [4] U. van Kolck, Lect. Notes Phys. **513** (1998) 62 [hep-ph/9711222].
  - [5] D. B. Kaplan, M. J. Savage and M. B. Wise, Phys. Lett. B **424** (1998) 390 [nucl-th/9801034].
  - [6] P. F. Bedaque, H.-W. Hammer and U. van Kolck, Phys. Rev. C **58** (1998) 641 [nucl-th/9802057].
  - [7] D. B. Kaplan, M. J. Savage and M. B. Wise, Nucl. Phys. B **534**, (1998) 329 [arXiv:nucl-th/9802075].

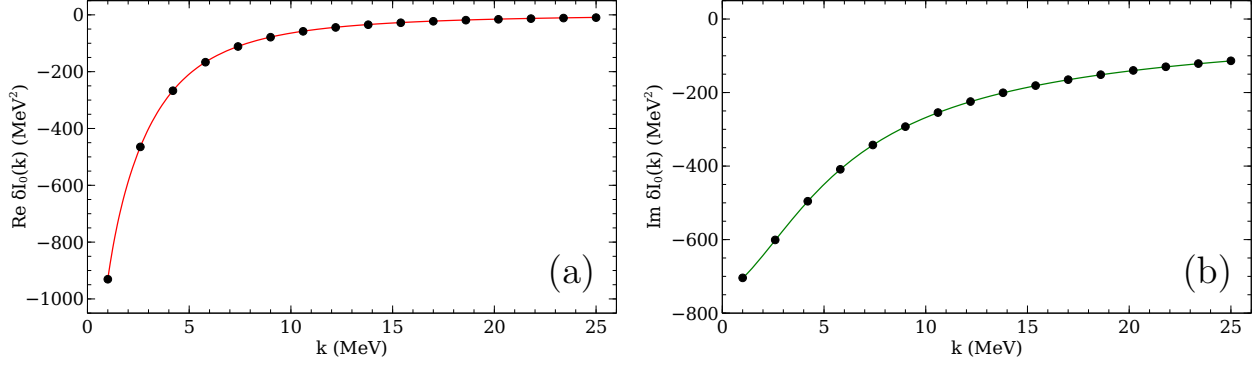


Figure 14: Numerical evaluation of  $\delta J_0(k)$ : (a) real part; (b) imaginary part. Black dots correspond to the integral given in Eq. (A52). The solid lines show the functions defined in Eqs. (A53) (a) and (A55) (b). The calculation was performed with an explicit small imaginary part of  $\varepsilon = 0.05$  MeV added to the real momentum  $k$  and a momentum cutoff of 16000 MeV.

- [8] M. C. Birse, J. A. McGovern and K. G. Richardson, Phys. Lett. B **464** (1999) 169 [hep-ph/9807302].
- [9] U. van Kolck, Nucl. Phys. A **645**, (1999) 273 [arXiv:nucl-th/9808007].
- [10] J.-W. Chen, G. Rupak and M. J. Savage, Nucl. Phys. A **653** (1999) 386 [nucl-th/9902056].
- [11] P. F. Bedaque and H. W. Griesshammer, Nucl. Phys. A **671** (2000) 357 [nucl-th/9907077].
- [12] F. Gabbiani, P. F. Bedaque and H. W. Griesshammer, Nucl. Phys. A **675** (2000) 601 [arXiv:nucl-th/9911034].
- [13] L. H. Thomas, Phys. Rev. **47** (1935) 903.
- [14] P. F. Bedaque, H.-W. Hammer and U. van Kolck, Nucl. Phys. A **676** (2000) 357 [arXiv:nucl-th/9906032].
- [15] H.-W. Hammer and T. Mehen, Nucl. Phys. A **690** (2001) 535 [nucl-th/0011024].
- [16] H.-W. Hammer and T. Mehen, Phys. Lett. B **516**, 353 (2001) [nucl-th/0105072].
- [17] P. F. Bedaque, G. Rupak, H. W. Griesshammer and H.-W. Hammer, Nucl. Phys. A **714** (2003) 589 [arXiv:nucl-th/0207034].
- [18] I. R. Afnan and D. R. Phillips, Phys. Rev. C **69** (2004) 034010 [nucl-th/0312021].
- [19] H. W. Griesshammer, Nucl. Phys. A **760** (2005) 110 [nucl-th/0502039].
- [20] A. C. Phillips, Nucl. Phys. A **107** (1968) 209.
- [21] V. Efimov, Phys. Lett. B **33** (1970) 563.
- [22] V. Efimov, Nucl. Phys. A **362** (1981) 45.
- [23] H.-W. Hammer and L. Platter, Ann. Rev. Nucl. Part. Sci. **60** (2010) 207 [arXiv:1001.1981 [nucl-th]].
- [24] J. Vanasse, Phys. Rev. C **88** (2013) 044001 [arXiv:1305.0283 [nucl-th]].
- [25] S. König and H.-W. Hammer, Phys. Rev. C **90** (2014) 3, 034005 [arXiv:1312.2573 [nucl-th]].
- [26] J. Vanasse, D. A. Egolf, J. Kerin, S. König and R. P. Springer, Phys. Rev. C **89** (2014) 6, 064003 [arXiv:1402.5441 [nucl-th]].
- [27] L. Platter, H.-W. Hammer and U.-G. Meißner, Phys. Lett. B **607** (2005) 254 [nucl-th/0409040].
- [28] J. Kirscher, H. W. Griesshammer, D. Shukla and H. M. Hofmann, Eur. Phys. J. A **44** (2010) 239 [arXiv:0903.5538 [nucl-th]].
- [29] J. Kirscher, Phys. Lett. B **721** (2013) 335 [arXiv:1105.3763 [nucl-th]].
- [30] J. Kirscher, *PhD thesis*, George Washington University, 2011 [arXiv:1506.00347 [nucl-th]].

- [31] I. Stetcu, B. R. Barrett and U. van Kolck, Phys. Lett. B **653** (2007) 358 [nucl-th/0609023].
- [32] N. Barnea, L. Contessi, D. Gazit, F. Pederiva and U. van Kolck, Phys. Rev. Lett. **114** (2015) 5, 052501 [arXiv:1311.4966 [nucl-th]].
- [33] S. R. Beane *et al.* [NPLQCD Collaboration], Phys. Rev. Lett. **115** (2015) 13, 132001 [arXiv:1505.02422 [hep-lat]].
- [34] J. Kirscher, N. Barnea, D. Gazit, F. Pederiva and U. van Kolck, Phys. Rev. C **92** (2015) 5, 054002 [arXiv:1506.09048 [nucl-th]].
- [35] E. Braaten and H.-W. Hammer, Phys. Rev. Lett. **91** (2003) 102002 [nucl-th/0303038].
- [36] E. Epelbaum, H.-W. Hammer, U.-G. Meißner and A. Nogga, Eur. Phys. J. C **48** (2006) 169 [hep-ph/0602225].
- [37] H.-W. Hammer, D. R. Phillips and L. Platter, Eur. Phys. J. A **32** (2007) 335 [arXiv:0704.3726 [nucl-th]].
- [38] X. Kong and F. Ravndal, Phys. Lett. B **450** (1999) 320 [arXiv:nucl-th/9811076].
- [39] X. Kong and F. Ravndal, Nucl. Phys. A **665** (2000) 137 [hep-ph/9903523].
- [40] X. Kong and F. Ravndal, Phys. Rev. C **64** (2001) 044002 [arXiv:nucl-th/0004038].
- [41] M. Butler and J. W. Chen, Phys. Lett. B **520** (2001) 87 [nucl-th/0101017].
- [42] T. Barford and M. C. Birse, Phys. Rev. C **67** (2003) 064006 [arXiv:hep-ph/0206146].
- [43] S.-I. Ando, J. W. Shin, C. H. Hyun and S. W. Hong, Phys. Rev. C **76** (2007) 064001 [arXiv:0704.2312 [nucl-th]].
- [44] S.-I. Ando, J. W. Shin, C. H. Hyun, S. W. Hong and K. Kubodera, Phys. Lett. B **668** (2008) 187 [arXiv:0801.4330 [nucl-th]].
- [45] S.-I. Ando and M. C. Birse, Phys. Rev. C **78** (2008) 024004 [arXiv:0805.3655 [nucl-th]].
- [46] G. Rupak and X. w. Kong, Nucl. Phys. A **717** (2003) 73 [nucl-th/0108059].
- [47] S. König and H.-W. Hammer, Phys. Rev. C **83** (2011) 064001 [arXiv:1101.5939 [nucl-th]].
- [48] J. Kirscher and D. R. Phillips, Phys. Rev. C **84** (2011) 054004 [arXiv:1106.3171 [nucl-th]].
- [49] S. Ando and M. C. Birse, J. Phys. G: Nucl. Part. Phys. **37** (2010) 105108 [arXiv:1003.4383 [nucl-th]].
- [50] L. P. Kok, D. J. Struik, and H. van Haeringen, Internal Report 151 (1979), University of Groningen.
- [51] L. P. Kok, D. J. Struik, J. E. Holwerda, and H. van Haeringen, Internal Report 170 (1979), University of Groningen.
- [52] S. König, *Effective quantum theories with short- and long-range forces*, Doctoral thesis (Dissertation), University of Bonn, 2013.
- [53] H.-W. Hammer and S. König, Phys. Lett. B **736** (2014) 208 [arXiv:1406.1359 [nucl-th]].
- [54] S. König, H. W. Griebhammer and H.-W. Hammer, J. Phys. G **42** (2015) 045101 [arXiv:1405.7961 [nucl-th]].
- [55] J. Kirscher and D. Gazit, Phys. Lett. B **755** (2016) 253 [arXiv:1510.00118 [nucl-th]].
- [56] H. W. Griebhammer, Nucl. Phys. A **744** (2004) 192 [nucl-th/0404073].
- [57] H. W. Griebhammer, M. R. Schindler and R. P. Springer, Eur. Phys. J. A **48** (2012) 7 [arXiv:1109.5667 [nucl-th]].
- [58] C. van der Leun and C. Alderliesten, Nucl. Phys. A **380** (1982), 261.
- [59] J. J. de Swart, C. P. F. Terheggen and V. G. J. Stoks, arXiv:nucl-th/9509032.
- [60] M. A. Preston and R. K. Bhaduri, *Structure of the Nucleus*, Addison-Wesley Publishing Company, Reading, MA (1975).
- [61] J. R. Bergervoet, P. C. van Campen, W. A. van der Sanden and J. J. de Swart, Phys. Rev. C **38** (1988) 15.

- [62] V. G. J. Stoks, R. A. M. Klomp, M. C. M. Rentmeester and J. J. de Swart, Phys. Rev. C **48** (1993) 792.
- [63] L. Platter, C. Ji and D. R. Phillips, Phys. Rev. A **79** (2009) 022702 [arXiv:0808.1230 [cond-mat.other]].
- [64] C. Ji, D. R. Phillips and L. Platter, Europhys. Lett. **92** (2010) 13003 [arXiv:1005.1990 [cond-mat.quant-gas]].
- [65] U. L. van Kolck, *PhD thesis*, University of Texas, 1993.
- [66] U. van Kolck, Few Body Syst. Suppl. **9** (1995) 444.
- [67] J. L. Friar, U. van Kolck, M. C. M. Rentmeester and R. G. E. Timmermans, Phys. Rev. C **70** (2004) 044001 [nucl-th/0406026].
- [68] D. E. González Trotter *et al.*, Phys. Rev. C **73** (2006) 034001.
- [69] V. Huhn, L. Watzold, C. Weber, A. Siepe, W. von Witsch, H. Witała and W. Glöckle, Phys. Rev. C **63** (2001) 014003.
- [70] J. L. Friar, B. F. Gibson and G. L. Payne, Phys. Rev. C **35** (1987) 1502.
- [71] R. A. Brandenburg, S. A. Coon, and P. U. Sauer, Nucl. Phys. A **294** (1978) 395.
- [72] L. Hostler and R. H. Pratt, Phys. Rev. Lett. **10** (1963) 469.
- [73] J. Meixner, Math. Z. **36** (1933) 677.
- [74] I. S. Gradshteyn and I. M. Ryzhik, *Table of Integrals, Series and Products*, 7th ed., Academic Press (2007), Eqs. 8.230.1 and 8.230.2.
- [75] J. C. Y. Chen and A. C. Chen, Adv. Atom. Mol. Phys. **8** (1972) 72.
- [76] J. Dušek, Czech. J. Phys. B **31** (1981) 941.
- [77] H. van Haeringen and R. van Wageningen, J. Math. Phys. **16** (1975) 1441.